# The Mouse Ileal Lipid-binding Protein Gene: A Model for Studying Axial Patterning during Gut Morphogenesis

**Michael W. Crossman,*‡ Sherrie M. Hauft,‡ and Jeffrey I. Gordon***

Departments of *Molecular Biology and Pharmacology and ‡Pediatrics, Washington University School of Medicine, St. Louis, Missouri 63110

***Abstract.*** Normal, chimeric-transgenic, and transgenic mice have been used to study the axial patterns of ileal lipid-binding protein gene (*Ilbp*) expression during and after completion of gut morphogenesis. *Ilbp* is initially activated in enterocytes in bidirectional wave that expands proximally in the ileum and distally to the colon during late gestation and the first postnatal week. This activation occurs at the same time that a wave of cytodifferentiation of the gut endoderm is completing its unidirectional journey from duodenum to colon. The subsequent contraction of *Ilbp*'s expression domain, followed by its reexpansion from the distal to proximal ileum, coincides with a critical period in gut morphogenesis (postnatal days 7–28) when its proliferative units (crypts) form, establish their final stem cell hierarchy, and then multiply through fission. The wave of reactivation is characterized by changing patterns of *Ilbp* expression: (*a*) at the proximal most boundary of the wave, villi contain a mixed population of scattered ileal lipid-binding protein (ILBP)-positive and ILBP-negative enterocytes derived from the same monoclonal crypt; (*b*) somewhat more distally, villi contain vertical coherent stripes of wholly ILBP-positive enterocytes derived from monoclonal crypts and adjacent, wholly ILBP-negative stripes of enterocytes emanating from other monoclonal crypts; and (*c*) more distally, all the enterocytes on a villus support *Ilbp* expression. Functional mapping studies of *Ilbp*'s promoter in transgenic mice indicate that nucleotides −145 to +48 contain *cis*-acting elements sufficient to produce an appropriately directed distal-to-proximal wave of *Ilbp* activation in the ileum, to maintain an appropriate axial distribution of monophenotypic wholly reporter-positive villi in the distal portion of the ileum, as well as striped and speckled villi in the proximal portion of its expression domain, and to correctly support reporter production in villus-associated ileal enterocytes. Nucleotides −417 to −146 of *Ilbp* contain a "temporal" suppressor that delays initial ileal activation of the gene until the second postnatal week. Nucleotides −913 to −418 contain a temporal suppressor that further delays initial activation of the gene until the third to fourth postnatal week, a spatial suppressor that prohibits gene expression in the proximal quarter of the ileum and in the proximal colon, and a cell lineage suppressor that prohibits expression in goblet cells during the first two postnatal weeks.

THE mouse gut epithelium is an attractive model system for studying how regional diversity or axial patterning is established and maintained. Its four component cell lineages are rapidly renewed through a geographically well-organized sequence of proliferation, commitment, and migration-associated differentiation. This renewal occurs perpetually throughout the lifespan of the mouse and is fueled by a stem cell hierarchy that is maintained in an anatomically distinct unit known as the crypt of Lieberkühn. Morphogenesis of the gut epithelium occurs relatively late in development, from embryonic day (E)[1] 15 through postnatal day (P) 21 (1, 3, 9, 49). This allows the process of axial patterning (establishment of region-specific differences in the distribution and differentiation of its component cell lineages) to be studied in fetal and postnatal animals.

The mouse gut endoderm undergoes rapid remodeling from E15 to E19 as a proximal-to-distal wave of cytodifferentiation converts it from a pseudostratified to a simple columnar epithelium. This monolayer covers nascent villi that are separated from one another by a proliferative compartment

Address all correspondence to Jeffrey I. Gordon, Department of Molecular Biology and Pharmacology, Box 8103, Washington University School of Medicine, 660 South Euclid Avenue, St. Louis, MO 63110.

1. *Abbreviations used in this paper*: BrdUrd, 5'-bromo-2'-deoxyuridine; E, embryonic day; ES cell, embryonic stem cell; *Fabpi*, intestinal fatty acid binding protein gene; *Fabpl*, liver fatty acid binding protein gene; hGH, human growth hormone; GRE, glucocorticoid responsive element; HNF, hepatic nuclear factor; I-FABP, intestinal fatty acid binding protein; *Ilbp*, mouse ileal lipid binding protein gene; ILBP, ileal lipid binding protein; L-FABP, liver fatty acid binding protein; P, postnatal day; UEA-I, *Ulex europeaus* agglutinin type I.

known as the intervillus epithelium. The intervillus epithelium represents the precursor to intestinal crypts. Studies of mouse aggregation chimeras indicate that the intervillus epithelium is polyclonal, i.e., supplied by several active stem cells with distinct genotypes (68). A poorly understood process of cell selection occurs during crypt formation (3, 9), which converts them to monoclonality by P14. Crypt number is dramatically increased between the second and third postnatal week through fission (3, 9). The adult mouse small intestine contains ~1.1 million crypts (25), each of which is supplied by one or more active multipotent stem cells (22, 27, 41, 80). The descendants of these stem cells undergo several rounds of cell division in the lower and middle thirds of each crypt, forming a transit cell population (54). Cellular differentiation occurs during a bipolar migration along the crypt-to-villus axis. Enterocytes, goblet cells, and enteroendocrine cells differentiate as they are rapidly translocated in vertical coherent bands from a crypt to the apex of a surrounding villus (5, 7, 8, 67), after which they are exfoliated. Proliferation, upward migration/differentiation, and exfoliation are completed in 2–5 d (82). In contrast, Paneth cells differentiate during descent to the base of the crypt, where they reside for ~20 d (6).

Axial patterning of the mouse intestinal epithelium is evident at the time of its initial cytodifferentiation in late fetal life. Studies with E15 intestinal isografts implanted into the subcutaneous tissues of young adult syngeneic or nude mouse recipients indicate that this patterning can occur without exposure to normal luminal contents, e.g., the microflora, biliary and pancreatic secretions (17, 62, 63). The nature and location of the epithelium's positional address is unknown. Region-specific differentiation could reflect a cell autonomous process or it could be programmed/maintained by interactions between epithelial, stromal, and/or mesenchymal compartments.

The different cephalocaudal and developmental patterns of activation of three homologous fatty acid–binding protein genes in villus-associated enterocytes provide an opportunity for identifying *cis*- and *trans*-acting factors that regulate regional specification of the enterocytic lineage during gut morphogenesis (12, 56–60, 70, 74, 75). The intestinal fatty acid binding protein gene (*Fabpi*) is activated on E15. *Fabpi*'s expression domain is fully established by the first postnatal week and extends from the proximal duodenum to the proximal colon with highest steady-state levels of its mRNA and protein products occurring in the distal jejunum (12). The liver fatty acid binding protein gene (*Fabpl*) is also activated on E15 (26). Like *Fabpi*, its expression domain in the gut is established coincident with movement of the proximal-to-distal wave of endodermal cytodifferentiation (57). The concentration of liver fatty acid binding protein (L-FABP) mRNA and protein is highest in the proximal jejunum of suckling, weaning, and adult mice (56, 57, 70). The ileal lipid binding protein gene (*Ilbp*) encodes a protein that appears to be the cytosolic receptor for bile acids that have undergone sodium-dependent active transport into the enterocyte (37, 81). Its mRNA is confined to the ileum of adult mice and is not detectable in total cellular RNA prepared from the intact intestine until after birth (64). In the current study, we have characterized the developmental patterns of expression of the mouse *Ilbp* gene and *Ilbp*/reporter transgenes. The results have allowed us to identify *cis*-acting elements that regulate axial patterning of the distal small intestine during completion of gut morphogenesis and that are responsive to temporal factors that operate over a time scale of weeks to months.

## Materials and Methods

### Isolation of Mouse ILBP cDNA

An oligo (dT)-primed cDNA library was prepared in lambda ZapII (Stratagene, La Jolla, CA) using poly($A^+$) RNA isolated from the distal third of adult male FVB/N mouse small intestine. The library was screened with a full-length porcine ILBP cDNA (20, 64). 10 probe-positive recombinant phages were isolated with inserts ranging in size from 200 to 560 bp. The largest (560 bp) was subcloned into pBluescript SK($^-$) (yielding pMC4), and both strands were sequenced (66). Restriction endonuclease digestion and nucleotide sequence analyses of double-stranded cDNAs contained in the other recombinant phage revealed that they were all represented within pMC4's 560-bp insert.

### Isolation and Sequencing of the Mouse Ilbp Gene

An adult DBA/2J mouse liver genomic library (Clontech, Palo Alto, CA) was screened with the full-length ileal lipid-binding protein (ILBP) cDNA. Five unique probe-positive phages were recovered from the 300,000 plaques that were surveyed. The insert in one of these phages (λILBP.5) was analyzed further. Two apparently contiguous pieces of DNA consisting of a 3-kb EcoRI/BamHI fragment and a 4-kb BamHI/EcoRV fragment (Fig. 1 *A*) were each subcloned into pBluescript. The nucleotide sequences of both strands of these DNAs were determined using oligonucleotide primers and the dideoxynucleotide chain termination method. Two sets of oligonucleotide primers flanking the presumed junction between these two fragments were used together with λILBP.5 DNA for PCR: 5′-GCATGTATGTAAGTGCCTGG-3′ and 5′-GCTAGAGAGAGGGCTCAAG-3′ produce a 156-bp PCR fragment from both λILBP.5 and FVB/N spleen DNA while 5′-TAAACTGCCTTGTGGGTGC-3′ and 5′-AGAAATCTGCCTGCCTCTGC-3′ produce a 494-bp PCR product from the same template DNAs. These results allowed us to conclude that there were no additional sequences in this region of λILBP.5 DNA that were not represented in the 3-kb EcoRI/BamHI and 4-kb BamHI/EcoRV fragments. Intron/exon boundaries in mouse *Ilbp* were subsequently identified by comparing the deduced genomic sequence with the sequence of the 560-bp mouse ILBP cDNA.

### Primer Extension Analysis

To identify the start site of transcription of *Ilbp*, an oligonucleotide, 5′-GCGCTTCATGAACTCATCGT-3′, encoding $Asp^{16}$→$Arg^{21}$ of mouse ILBP (Fig. 1 *B*), was labeled with $^{32}P$ at its 5′ end (65) and annealed to total cellular RNA isolated from FVB/N ileum. Primer extension with avian myeloblastosis virus reverse transcriptase was carried out according to a previously published protocol (73). Negative template controls included yeast transfer RNA and mouse liver RNA. Reaction products were analyzed on urea-polyacrylamide sequencing gels, and their sizes were compared to the sizes of products obtained from sequencing the mouse *Ilbp* genomic clone with the same primer.

### Computer-assisted Sequence Analysis

Dot matrix comparisons were performed using the GCG software package (15). Quality scores >55 were considered potentially significant when using the Fit Consensus algorithm. Transcription factor databases (16, 21) were searched with the program supplied in Geneworks (IntelliGenetics, Mountain View, CA).

### Generation and Analysis of Transgenic Mice

***Construction of ILBP/hGH$^{+3}$ Fusion Genes.*** A 966-bp NcoI fragment, encompassing nucleotides −913 to +52 of mouse *Ilbp* was subcloned into NcoI-digested pBluescript KS, yielding pBSILO.9. pBSILO.9 was digested with BamHI/Ksp6321 yielding a 960-bp fragment spanning nucleotides −913 to +48. pBShGH is a recombinant pBluescript KS plasmid that contains the human growth hormone (hGH) gene beginning at its nucleotide +3 with all of its exons and introns ($hGH^{+3}$). pBShGH was linearized with BamHI, ligated to the 0.96-kb BamHI/Ksp6321 *Ilbp* fragment, and the remaining Ksp6321 end was filled in with Klenow fragment of DNA poly-

merase before a second, blunt end ligation reaction. This yielded pILhGH containing nucleotides −913 to +48 of mouse *Ilbp* linked to $hGH^{+3}$ ($ILBP^{-913\ to\ +48}/hGH^{+3}$). $ILBP^{-913\ to\ +48}/hGH^{+3}$ was excised from pILhGH using ScaI and EcoRI. $ILBP^{-417\ to\ +48}/hGH^{+3}$ and $ILBP^{-145\ to\ +48}/hGH^{+3}$ were obtained by digesting pILhGH with XcmI/EcoRI and AfI II/EcoRI, respectively. All $ILBP/hGH^{+3}$ fusion genes were purified by agarose gel electrophoresis followed by glass bead extraction (GeneClean II; BIO 101, Inc., Vista, CA) and passage through a 0.22-μm Ultrafree MC filter unit (Millipore Corp., Bedford, MA). Each purified preparation of DNA was adjusted to a final concentration of 5 ng/μl Tris-EDTA buffer (10 mM Tris, 0.2 mM EDTA, pH 7.4) for pronuclear injections.

***Pronuclear Injection and Identification of Transgenic Animals.*** FVB/N mice were obtained from Taconic Farms, Inc. (Germantown, NY). Purified pronucleus $ILBP/hGH^{+3}$ DNAs were injected into the pronucleus of fertilized FVB/N oocytes. Injected eggs were transferred to pseudopregnant Swiss Webster mice (30). Live born animals were screened at the time of weaning for the presence of the transgenes using the polymerase chain reaction, tail DNA as a template, and two oligonucleotide primers, 5′-GACCAACCTTCTTCCTTAAGCTGCTCGCTGC-3′ (sense primer representing nucleotides −1 to +29 of mouse *Ilbp*) and 5′-CGGGATCCCGGGCACTAACCCTCAGGTTTG-3′ (antisense primer representing nucleotides +351 to +332 of hGH; reference 69). The PCR mixture (total vol = 50 μl) contained Tris (20 mM, pH 8.55), $MgCl_2$ (2.5 mM), $(NH_4)_2SO_4$ (16 mM), bovine serum albumin (150 μg/ml), oligonucleotide primers (2 μM), dNTPs (100 μM), KlenTaq DNA polymerase (Ab Peptides), and mouse genomic (tail) DNA (1 μg). The following cycling conditions were used: denaturation = 1 min at 94°C, annealing = 2 min at 56°C, and extension = 2 min at 72°C for a total of 30 cycles. Each of the three $ILBP/hGH^{+3}$ transgenes yields a 205-bp amplified product with these primers.

***Calculation of Transgene Copy Number.*** Transgene copy number was determined by Southern blot analysis of genomic DNA prepared from the liver or spleen of $F_1$ or $F_2$ mice. 10 μg of DNA was digested with PvuII, which produces a 1-kb internal fragment from each $ILBP/hGH^{+3}$ transgene. The PvuII digests were fractionated by agarose gel electrophoresis and transferred to nylon membranes (GIBCO/BRL, Gaithersburg, MD). Southern blots were probed with a $^{32}P$-labeled, 150-bp BglII/PvuII fragment obtained from exon V of hGH (74). The intensity of the hybridization signal was quantitated by a storage phosphorimaging system (Molecular Dynamics, Sunnyvale, CA). Signal intensities produced from PvuII-digested genomic DNA were compared to those obtained from known amounts of PvuII-digested pILhGH DNA included as internal standards in each blot. Only signals in the linear range of film sensitivity were used to calculate copy number.

***Maintenance of Mice.*** Each transgenic pedigree was established and subsequently maintained by crosses to normal FVB/N littermates (Table I). All mice were caged in microisolators and kept under a strictly controlled light cycle (lights on at 0600 h, off at 1800 h). Animals were given a standard autoclavable chow diet (no. 5010; Ralston Purina, St. Louis, MO) ad libitum. The mice used in this study were free of pathogens including murine hepatitis virus. For developmental studies, gestational age was calculated from the day a vaginal plug was first noted (designated day 0). Postnatal age was computed with day 1 equal to the day of birth.

## *Analysis of the Developmental, Cellular, and Axial Patterns of $ILBP/hGH^{+3}$ Expression*

***Measurement of ILBP and hGH mRNA Levels in Normal and Transgenic Mice.*** FVB/N mice were killed between 1200 and 1400 h at E15, E16, E17, E18, P2, P5, P7, P9, P11, P13, P15, P17, P19, P28, P42, and P84 ($n$ = 8 mice from one litter for each fetal time point surveyed; $n$ = 2 littermates for each postnatal time point). For E15–E18 mice, the entire length of the intestine (i.e., from the gastroduodenal junction to the rectum) was removed en bloc, frozen in liquid nitrogen, the pooled samples from each time point were pulverized, and RNA was extracted with RNAzol (10). For postnatal time points, the small intestine was divided into three equal-length segments (designated duodenum, jejunum, and ileum). The cecum was removed by making incisions at the ileal-cecal and cecal-colonic junctions, and the colon was divided into two equal-length portions (proximal and distal colon). Comparably positioned segments of gut were pooled from each of the two littermates killed at each postnatal time point surveyed, and total cellular RNA was recovered.

Transgenic mice and their normal littermates were killed by cervical dislocation between 1200 and 1400 h at P7, P14, P21, and P28. Their gastrointestinal tracts were rapidly subdivided into seven segments (stomach, duodenum, jejunum, ileum, cecum, proximal, and distal colon). Each segment of gut was snap frozen in liquid nitrogen. 11 additional tissues were also obtained from each mouse (brain, submaxillary glands, thymus, heart, lung, kidney, liver, spleen, pancreas, adrenal, and gonads). Total cellular RNA was extracted from frozen pulverized tissue using RNAzol.

Samples of total cellular RNA (10 μg) were fractionated by denaturing formaldehyde-agarose gel electrophoresis (65) and were transferred to nylon membranes. Each blot contained ILBP and hGH mRNA standards (0.1–500 pg) prepared by in vitro run-off transcription (47). Blots were sequentially probed with three $^{32}P$-labeled (18) DNAs: (*a*) the 150-bp hGH exon V fragment; (*b*) a 540-bp PstI/EcoRV fragment encompassing the full-length mouse ILBP cDNA from pMC4; and (*c*) an 870-bp RsaI fragment from human glyceraldehyde-3-phosphate dehydrogenase cDNA (pHcGAP; American Type Culture Collection, Rockville, MD). Washed blots were subsequently scanned using a storage phosphor imager to calculate the steady-state levels of specific mRNAs. Labeled probe was removed by incubating the blot at 100°C for 5 min in 0.01× SSC/0.01% SDS. The stripped blot was then reprobed with the next $^{32}P$-labeled DNA.

***Single- and Multilabel Immunocytochemical Studies.*** Normal FVB/N mice were killed by decapitation at E18 and by cervical dislocation at P2, P5, P7, P9, P11, P13, P15, P17, P19, P21, and P28 ($n$ = 2–4 littermates/time point). Transgenic mice and their normal littermates were killed at P7, P14, P28, P48, P56, P70, P84 (12 wk), and P168 (24 wk) by cervical dislocation ($n$ = 2 transgenic mice and 1–2 normal littermates/time point per pedigree). Pregnant mice and postnatal animals received an intraperitoneal injection of an aqueous solution of 120 mg/kg 5′-bromo-2′-deoxyuridine (BrdUrd) and 12 mg/kg 5′-fluoro-2-deoxyuridine 90 min before death to label proliferating cells in S phase. E18 mice were fixed directly in Bouin's solution after making an incision in their anterior abdominal wall to expose the viscera. After washing in 70% ethanol, the intact embryo was divided in half along its sagittal plane, embedded in paraffin, and sectioned along its cephalocaudal axis. For all postnatal mice, the entire gastrointestinal tracts were removed en bloc and fixed in Bouin's solution for 12–24 h and were then washed in 70% ethanol. For P2–P13 mice, Swiss rolls (29) of the entire intestine were embedded in paraffin. For ⩾P14 animals, Swiss rolls were prepared from each intestinal segment, i.e., duodenum, jejunum, ileum, cecum/proximal colon, and distal colon. Bouin's fixed samples of brain, lung, heart, thymus, stomach, pancreas, liver, spleen, adrenal, and gonads were also analyzed from these mice.

5-μm thick sections were cut, deparaffinized, rehydrated in PBS (pH 7.4), and incubated in PBS-blocking buffer (BSA [1%]), powdered skim milk (0.2% wt/vol), and Triton X-100 (0.3%) for 15 min at room temperature. Primary antisera were diluted in PBS-blocking buffer and incubated overnight at 4°C. Slides were then washed in PBS. Antigen-antibody complexes were subsequently detected using (*a*) gold-labeled secondary antibodies with silver enhancement (56); (*b*) Texas red- or CY3-labeled donkey anti-goat secondary antibodies; and/or (*c*) fluorescein-labeled donkey anti-rabbit secondary Ig. (All secondary antibodies were obtained from Jackson ImmunoResearch Labs., Inc. [West Grove, PA] and diluted 1:500 in blocking buffer.) Slides were washed in PBS and mounted in PBS/glycerol (1:1 vol/vol). The final dilution and sources of these primary antisera were rabbit anti-ILBP (1:2000; see below), rabbit anti-I-FABP (1:2000; reference 42), rabbit anti-L-FABP (1:2000; reference 42), goat anti-hGH (1:2000; reference 45), goat anti-BrdUrd (1:1000, reference 11), and goat or rat anti-serotonin (1:1000; Incstar). FITC-labeled *Ulex europaeus* agglutinin-I (UEA-I), which detects fucosyl-α-2-galactosyl-β linked glycoconjugates (71), was obtained from Sigma Immunochemicals (St. Louis, MO), diluted 1:500 in PBS-blocking buffer (minus powdered skim milk), and used to identify goblet cells in FVB/N ileum and distinguish them from enterocytes (17). The specificities and immunostaining characteristics of all members of the antibody/lectin panel have been extensively characterized in the gastrointestinal tracts of normal and transgenic mice (12, 17, 36, 57, 58, 70, 74, 75, 77). Moreover, control experiments established that (*a*) none of the labeled secondary antibodies bound to tissue sections in the absence of primary antibody or in the presence of preimmune sera; (*b*) none of the normal FVB/N mouse tissues gave a detectable signal when incubated with the anti-hGH sera followed by a fluoroprobe-tagged secondary antibody; and (*c*) overnight incubation of a 1:2000 dilution of anti-hGH sera with hGH (1 μg/ml; Boehringer Mannheim Biochemicals, Indianapolis, IN) completely blocked its ability to react with gut cell lineages in mice that expressed the various $ILBP/hGH^{+3}$ transgenes (data not shown).

***Confocal Microscopy.*** A Molecular Dynamics Multiprobe 2001 inverted confocal laser scanning confocal microscope system equipped with a 60× oil immersion objective lens with a numerical aperture of 1.4 was used to scan sections of Bouin's fixed ileum prepared from P7 $ILBP^{-145\ to\ +48}/hGH^{+3}$ transgenic mice and their normal littermates. These sections were

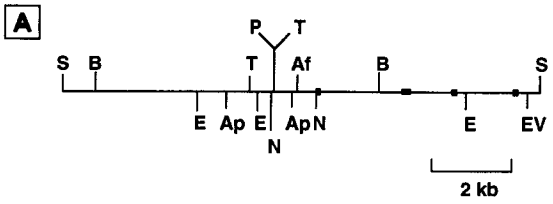


B

```
aattctaggattggagactaaagactgctatgtgtgcgtcaaagttgacttttcatcaggtcaggaggcagtgagtcaggggctggctcagtagagaaaggtacttggtgccaggctac -931
acacacacacacacacacacatggtacacgtgtaaacacataagagagacagacagacagacagacagacagagagagagagagagagagagagagagagagagaatcgactatccctgg
tcccaggtagggagtcagccagtgtggtcaattctgctttgaatagaaatgatgggatttcacagagagaagacccccagaacaggagagggtttttttttgtttgtttgtttgttttgtt -691
ttttgttttttgttttttttttttcttgcttgttgcttgcttgcttgcttttggtttgttcctgatacaggatcttgctctgtgaccccattcttttccttggcattatgacaaaccttctt
cagcctcccaagtacccaggattatcggtgtcgtccacagtgcccaggcgaaacttttgtcattaacagtagtaatggtgaagatgctgacgagggattttgcattgcttctttaagtgacc -451
cagaagccacccccacacccccaaagactggaaccccatgtgtaaagtggcacataagcatctagcttacaaacttcacttgtgtgccttgggtcagggttggcctgggggctcccctggga
aaggctcatgccttgttcttctggattgccatatacagttcagtgccacagagcttggtaaatgaaggctgaggagagcttagggatgggcagagagggggctgagcagagaggtgaatgac -211
cacactctgtggccgtcctggccttggccttactgggactggtagtgggattgtaggtgttttcctaaggtgaataaccttggggctcctgcccacgtcataaaatatcaagcaactc
ctgctagggcaggactgagaagtggggtgacttggggctgagccttggcagttgggagtgttataagctgggactccagacttcctcaggACCAACCTTCTTCCTTAGCTGCTCGCTGC 29
TGCCAGCTCTCTTCCAGCACC ATG GCC TTC AGT GGC AAA TAT GAA TTT GAG AGT GAG AAG AAT TAC GAT GAG TTC ATG AAG CGC CTG G gtgagt 123
                      M  A  F  S  G  K  Y  E  F  E  S  E  K  N  Y  D  E  F  M  K  R  L  G
gagcttctttgtgtccttcccgggactggctgcttatagctagctctgggataggaacccaaactcttggggtagagtaggacagaactcatccatccatccttccatccatccatcc 243
atccttccatccatccatccatccatccatccatccatccacccaccaccagactttgctgagcaaacactctgttctgtctctaaagataatcaaagctgtaacacatcctttgat
ttttaaaagacttagagaatttagtatctctaattcatgtacggaaagtgtgagtctcagacaagtttcatcaacattaaaggccacatagtagtgactggtgaagtggagatctgatg 483
tttattcgttcaaatgtttgttattgttgttgttattagaagcagggtctcatgcagtctaagctggcctcaaaatcactatgtagctgaggatgacgctgaaatcttgattccttggct
tctctctcagagggagggattacaggcatatgcatacctttgtgttatgtagtgctggtgaccacacctgggcttcactcatgctaggcgagcggtttcgtcaatcgagcctatccctaat 723
cctgctcaaagttattgaatgtctgctacatgcaaaggctgtcccaataattgggtttttttttttaatgtttttaaacgtgccatctctccagcccactgtcccaatattcttgatgagc
cacctcagagtgatttacctaagtcagtgacagaggtcattaacacccagaacccctgtcataaatgatgtcactatatcctgctagggagagatgaccaaggagttaatacagaaaccat 963
gtttaacaagacaatccacatagctcaccaacaaacttctcttcttcccttactgtactatttcgggtagagaaaccagatttattattattattattattattattattattattat
tattattattattatcattattacttgccttttgacagcaaaaggtctgtttcgagttgaccttgacactggtcagttgccaaagtgtcaaaggaaagtggatttgatggtcttgtcaa 1203
cctttcagtgcactagcactgaggccatgcaattgtcaaggatgagatgtagctctggtgggagacagtttgcttagcatgcctgaggccctgtttcaatcaccagcactgcataaacta
ggccttgtagtgagtgcctataatcccagcattcaggagactgcggaaggaaggccagaaattcaaggtcatccactgtccaggtcacttgggactatcaaaaaaaaaaaaaaaaaaaag 1443
gaaggaagaacagttccagtttcatgagacccacgggcatcctctttgtggtgtttgtccttctgctgtgtcagagtggcccgaaagtggagccccgtcccctctgtcctgtaa
ggccttgtggacaggctactttttcttctgagtctttatttcttttggtgtgtgtcataagatttatttatctttttatatctgttagagtttgcctgcatgtatgtaagtgcctggagtc -1683
cccagaggtcagaagaggtcactagagtccttacaacggtagttacagatggctgtaaactgccttgtgggtgctgggatccaaacccctgtaagagcagaaagtattcttaactcttgag
cctctctctagccccaggtcttataaaatagaaacattagaagactcaatctgaaaggttgcattcattccaaaatttcctgggcttggcaagtttttgcaatatgatatattactg 1923
taggaagatttgttatttttttaattaggatttttaacgtatgtgagtgcttttctcttatgcatgtctccttaccagtgttacagaaggttgtggggagccatgtgagtgctgggaatt
gaaccaggtcctctgtaacaagtacttttaactgatgagccatctcccagaccccacaatttgctgttattgaagagccaccaagggggggagagatggctcagcagttaagagtacc 2163
gacttcgccgggcatggtggcgcacgccttaatcccagcacttgggaggcagaggcaggcagatttctgagttcgaggccagcctggtctacaaagtgagttccaggacagccagggact
atacagagaaacccctgtttcgaaaaaccaaaaaaaaaaaaagagtaccgacttcttctaaaaggtgctgagttcaaatcccagcaaccacacagtgccttaccactatttgtaatgagatc 2403
tgatgcctcttctggggtgtctgaagacagctacagtgtacttatatataataaataaataaatcttaaaaaagaaagaaagaaagaaagaaagaaagaaagaaagaaagaaagaaaga
aagaaagaaaggtgaagaggaccaggtggttgggaggagatgtgagtggcacaaactctcacatttatgcttgcattatctctgtggggtggacctactgtcaccattttgtgagcac 2643
aaacacagtgagacagtgctctgcacaaacactggtctctctcattgcagagctgggcttgaagcatgtgctgtctatgtctcagtcactgtattcagcccccgcagggagcctgcctc
tggggaggaaatctcctccaccaaatcacagggctataagtagaccccatgtgttctctctgcttgtcactgggcccagGT CTT CCA GGA GAC GTG ATT GAA AGG GGA CG 2873
                                                                                    L  P  G  D  V  I  E  R  G  R
T AAC TTC AAG ATC ATC ACA GAG GTC CAG CAG GAC GGA CAG GAC TTC ACC TGG TCC CAG TCT TAC TCT GGG GGC AAC ATT ATG AGC AAC AA 2963
  N  F  K  I  I  T  E  V  Q  Q  D  G  Q  D  F  T  W  S  Q  S  Y  S  G  G  N  I  M  S  N  K
G TTC ACC ATT GGC AAA GAA TGT GAA ATG CAG ACC ATG GGG GGC AAG AAG TTC AAG gtgagagaccccctggctgccttctctgtgcttccccaggccagaagt 3064
  F  T  I  G  K  E  C  E  M  Q  T  M  G  G  K  K  F  K
cagcttctctatttcagatatgagcctctgctccccagattgagccttcagcacgaactctcttacctggtaacttcatgtttctgttgggtaatggctgccattagcaggaaacacaa 3184
ccaagacagatacaaatggctgctactacactgggtgtggcagtgcacaacattaatcccaggacttggggttcagagttctgggccaatctggtctacatagttctgggacagccgaaa
ggatatacagaaatcctgtctcaagaaacaaacaaacaaaaaagcagctgagcatttaatgtaactcacctcacttactgaatagtctatctatctatctatctatctatctatctatct 3424
atctatctatctatctatctatctattatctatctatctatctattatctatctatctatctatctatctatctatctattatctatctatctatctatctatctatctatctaatct 3664
acctatccatctacatctctctatcatctctctatctgttcatctgtctgtcatctatgtctccagcgagggtggtgtggtatgggggtggtgttagggggcatacactgccatgaccag
ccccccacttttattgagttctgtggacctaaactccagtctctttaccccactgaacaaactccccgctatcctcatgttttgagaacctgggccatggcaggcaatcactctgtcca 3904
ccaagccagctctacatgtgttaatttaaaaacgatctaagcgatgccaaaacaggttcattaggccgtgactagaggcttcatgttgaatgcttcatctctctctgcag GCT ACC GT 4021
                                                                                                                A  T  V
G AAG ATG GAG GGT GGC AAG GTG GTG GCA GAG TTC CCC AAC TAT CAC CAG ACT TCG GAG GTC GTG GGT GAC AAG TTG GTG GAG gtgagtgtgc 4113
  K  M  E  G  G  K  V  V  A  E  F  P  N  Y  H  Q  T  S  E  V  V  G  D  K  L  V  E
aaaagttctgactatttctatttaaagaggtgctcggtgaggctcaagggcagcctacagcttgcctcaggtcatagagctagtacttttgtggaggtaagacccattccagctgacatca 4233
agaggacattctcagccttttctagaggattagtgggcccctgccacactaccatgcttcttttctcagaatgaaaatacatctaatcatggtggcaaatgcctgcaatctcaacactctg
gaggccaagccaggaggatcttgaattccaagtcagcctggcacagagtgagacactgacccaaaatcacacacatacacacactctctctctctctctctctctctctctctct 4473
ctcacacacacacacacacacacacacacacacagcgggagagagagggggtgtgtgtgtcttagtgaaaagtgcatgtctacctgcatgaggttcaagtcttagtactgtcaaaatcaagtaag
aatttgaaaaccaacgaagtggtgttgaagcattgaaaaagaaaaaaacaaaaacaaaaacaaaaacaaaacaaaacaaaacaaaacaaaacgaggccaaaggtaaaggggcttgcagccaa 4713
gtctgaggatctgagttcaattccccgggaccacatgatggaaggtgagcactaactcctggctgctggctgtagtctgacttccacatgcatgctgttttcattcatacacataggaaa
agaatcaaagttagtatctctctgctgtgggtgaaaactggccattcaaagtggcctgaacacttttaatgaaaggtcagtcagtggtgctgatttccaaagcaatgttcccaggcc 4953
tgaggtgtgcaggaagagctgagggcaggagatgtggagcagcaggttgtgtccaaaagacttaatcttcaaacactgaaccaacccctcagtttgctcctctgtataatgggaacaacca
cctgggactcttgggaattagagatggaatagtgtgaaaagaggcctggcatatgcagtggtcaaaaggaacggtgatagcatgggggctaacatgcctacagccatcactttgcccct 5193
atttagcgtcttaacacatttctctcttcagtgtgactccggtaactgacagggaatctaagttccagaaagcagtgtgcctgccttgcacccatttagtaatgacagtagtggctagcct
tcctcagccgcacccctcaatcccaccatcgccactgtctggggaagtacactgactccctctgatctggtttctgctttcag ATC TCC ACC ATC GGG GAT GTG ACC TAT 5424
                                                                                        I  S  T  I  G  D  V  T  Y
GAG CGC GTA AGC AAG AGG CTG GCT TGA gctaccaggctgggcttggaggggctacgacccaccaataaaagtgtttcatggatcaccactgctagcccccagagtttctttg 5535
E  R  V  S  K  R  L  A  *
tttctgtttccgggagtcttccggcagcccctgcccaaatgggagcagggaaacatttaaggatcgctgagcaggccaaatgttggcctgggatgcctgaggttctctaccaaggcagag 5655
ggaggtgtggatgttgaatgtgggtgcagtgctatgtccttggaagcagccacaggtggagtgccgtggcacatttctgcg 5737
```

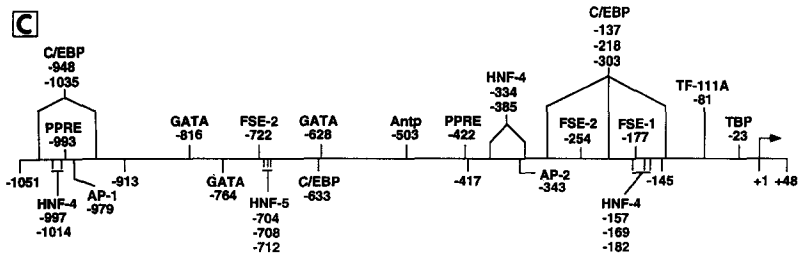


*Figure 1.* The sequence of mouse *Ilbp* and its protein product. (*A*) Restriction map of the DBA/2J mouse *Ilbp* locus. The filled-in boxes (■) represent exons 1–4. *Af*, AflII; *Ap*, ApaLI; *B*, BamHI, *E*, EcoRI; *EV*, EcoRV; *N*, NcoI; *P*, PmlI; *S*, SalI; *T*, TfiI. (*B*) Nucleotide sequence of mouse *Ilbp*. Exonic sequences are designated by upper case letters. The start site of transcription (nucleotide +1 = A) was determined by primer extension analysis. A predicted glucocorticoid response element (GRE) in intron I is underlined. The *Ilbp* gene sequence is available from EMBL/Genbank/DDBJ under accession number U00938. (*C*) Both strands of *Ilbp*'s 5′ nontranscribed domain were searched using an algorithm included in Geneworks, for sequences that match published consensus transcription factor binding sites. *HNF*, hepatic nuclear factor; *PPRE*, peroxisome proliferator receptor element; *C/EBP*, CAAT enhancer binding protein; *Antp*, *Antennapedia* homeobox element; *FSE*, fat-specific element, *TBP*, TATA box binding protein.

stained as described in the legend to Fig. 9 and were scanned using a confocal optical plane of 0.6 μm.

***Generation and Characterization of a Rabbit Anti-ILBP Sera.*** Porcine ILBP was expressed in and purified from *Escherichia coli* as previously described (64). The purity of the protein preparation was established by SDS-PAGE and by automated sequential Edman degradation. The purified protein was emulsified with Freund's complete adjuvant (Sigma Immunochemicals) and used to immunize New Zealand white rabbits.

The specificity of the resulting antisera was established by Western blot analysis. Jejunum, ileum, cecum, colon, lung, and liver were recovered from P7 and P42 FVB/N mice and were washed with ice cold 0.9% saline before freezing in liquid nitrogen. After lyophilization for 24 h at −60°C, the tissues were ground to a fine powder and resuspended in extraction buffer (30 mg dry wt of tissue/ml of Tris [0.125 M, pH 6.8], SDS [4%], β-mercaptoethanol [10%], glycerol [20%], aprotinin [5 μg/ml], phenylmethylsulfenyl fluoride [0.5 mM], leupeptin [5 μg/ml], pepstatin A [1 μg/ml], and EDTA [5 mM]). The suspension was boiled for 5 min and then spun for 5 min in a microfuge at room temperature to remove insoluble debris. The protein content was determined on the supernatant fraction (52). Solubilized tissue protein (50 μg) was fractionated by electrophoresis through 15% polyacrylamide gels containing 0.1% SDS (38) and was then transferred to nitrocellulose membranes using an electroblotting apparatus. Western blots were incubated at room temperature for 1 h with rabbit anti-ILBP diluted 1:1000 in Blotto (5% [wt/vol] nonfat dry milk, antifoam A (0.03%), Tween 20 [0.04%], sodium azide [0.1%], NaCl [0.15 M], and Tris [10 mM, pH 7.5]). The protein blots were subsequently washed in Blotto and antigen-antibody complexes detected with [$^{125}$I]protein A (1 μCi/ml Blotto). A single immunoreactive protein of the expected mass (14 kD) was present in the ileum and cecum, but not in the jejunum, lung, or liver of P7 and P42 animals (data not shown). Pretreatment of the antisera with purified ILBP completely blocked its ability to produce a signal when incubated with a duplicate blot.

The rabbit anti-ILBP serum was also incubated overnight in PBS with or without purified ILBP (1 μg/ml serum), and then applied to sections of Bouin's fixed ileum prepared from P28 FVB/N mice. The signal was completely abolished when the serum was pretreated with the purified antigen (data not shown).

## *Intestinal Isografts*

Intestinal isografts were prepared from E15 FVB/N mice (63). The entire small intestine plus cecum and colon were implanted into the dorsal subcutaneous fascia of P42 FVB/N male recipients (1 graft/recipient). 2 wk after implantation, mucoid material was aspirated from the lumen of each isograft using a sterile syringe. Isografts ($n$ = 2) were subsequently harvested 6 wk after implantation. The luminal fluid obtained from each isograft at the time of its recovery was devoid of bacteria as determined by Gram stain and by culture on Luria agar at 37°C under aerobic and anaerobic conditions (17). Duodenal, jejunal, ileal, and colonic segments from the grafts were fixed in Bouin's solution.

## *Generation of Chimeric-Transgenic Mice*

D3 embryonic stem (ES) cells (23) were used at passages 8–11 and maintained on mouse embryonic fibroblasts. 10 μg of HindIII-digested pLNDon DNA, containing nucleotides −596 to +21 of *Fabpl* linked to the hGH gene beginning at its nucleotide +3 (L-FABP$^{-596\ to\ +21}$/hGH$^{+3}$) followed by a neomycin selection cassette in the same transcriptional orientation (29), were introduced into ES cells by electroporation. Stably transfected, G418-resistant clones were isolated and Southern blot hybridization plus PCR analysis of their genomic DNA used to establish that complete integration of L-FABP$^{-596\ to\ +21}$/hGH$^{+3}$/neo had occurred. Chimeric-transgenic mice were generated by injecting 10–12 ES cells into 3.5 d postcoitum C57BL/6 blastocysts (2).

C57Bl/6 (control), 129/Sv (control), and C57Bl/6↔D3(pLNDon) chimeric-transgenic mice were killed at 12 wk of age by cervical dislocation, the entire intestine was removed en bloc, flushed with cold PBS, followed by Bouin's solution. The gut was then fixed in Bouin's for 6 h. Swiss rolls of the entire intestine were prepared for single and multilabel immunocytochemical analyses.

# *Results*

## *Mouse Ilbp Has an Organization Similar to that of Other Members of the Fabp Family*

Fig. 1 *B* shows the sequence of mouse *Ilbp* including 1051 nucleotides of its 5′ nontranscribed domain and 285 nucleotides of its 3′ flanking region. Like other members of the *Fabp* family, *Ilbp* contains four exons (117, 176, 89, and 54 bp) and three introns (2726, 995, and 1295 bp). Exon size and intron location are similar to that encountered in other family members (13, 24, 32, 72). Primer extension analyses using adult FVB/N ileal RNA as a template revealed that *Ilbp* has a single start site of transcription located 23 bp downstream from a TATA box (Fig. 1 *B*). Nucleotides −1051 to −1 of mouse *Ilbp* contain a number of sites that are similar to published consensus sequences for the binding of transcriptional factors (Fig. 1 *C*).

ILBP mRNA contains an open reading frame of 384 nucleotides encoding a protein of 128 amino acids which has 95% primary sequence identity with the orthologous rat protein (19, 34) and 70% identity with porcine ILBP (20).

Southern blot analysis performed using a variety of hybridization and washing stringencies indicate that *Ilbp* is a single-copy gene (data not shown). Mapping studies using a *M. spretus* panel disclosed that *Ilbp* is located on mouse chromosome 11, 10.2 cM from *Emvl4*, a retroviral insertion site (Birkenmeier, E. H., and J. I. Gordon, unpublished observations). *Ilbp* is not linked to any other *Fabp* family members or to other reported mapped genes encoding proteins involved in lipid metabolism and/or bile acid transport.

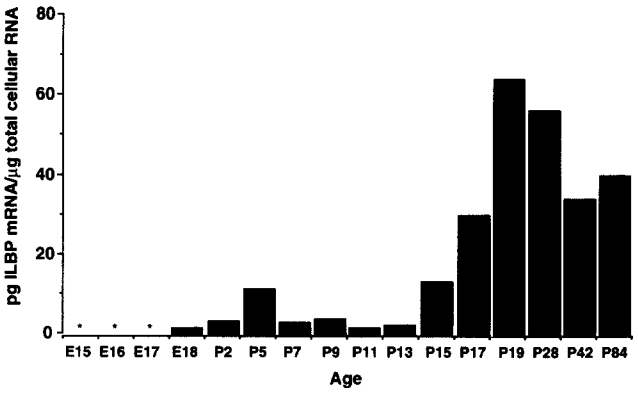


*Figure 2.* Developmental changes in ileal ILBP mRNA levels. mRNA concentrations were determined using RNA prepared from the entire intestine of E15–E18 mice ($n$ = 8 littermates/time point). Total cellular RNA was isolated from the distal third of the small intestine for all of the postnatal time points surveyed ($n$ = 2 littermates/time point). Note that tissues from littermates were pooled before RNA extraction.

### *Ilbp Is Only Expressed in the Ileum of FVB/N Mice and Undergoes a Complex Pattern of Activation during a Critical Period of Gut Morphogenesis*

Surveys of E15–E18 FVB/N mice indicated that ILBP mRNA was first detectable in total intestinal RNA at E18 (Fig. 2), coinciding to the time that the proximal-to-distal wave of cytodifferentiation of the pseudostratified gut epithelium to a monolayer has reached the ileum. Throughout postnatal development, a unique 600-nucleotide ILBP mRNA is confined to the distal third of the small intestine and cecum, i.e., the mRNA is not detectable in duodenal or jejunal RNAs prepared from P2–P84 mice, nor is it detectable in any of the 12 extraintestinal tissues surveyed. Steady-state levels of ileal ILBP mRNA rise from P2 to P5 and then fall abruptly (Fig. 2). Beginning at the suckling/weaning transition (P13), mRNA concentrations rise rapidly to a peak value of 65 pg/μg total ileal RNA on P19. Levels remain constant throughout weaning (P19–P28), and they fall slightly as animals reach sexual maturity (~35 pg/μg at P42). The concentration of this mRNA remains essentially unchanged at least through the next 5 mo of postnatal life (Fig. 2 and data not shown).

Single- and multilabel immunocytochemical analyses reveal a distal-to-proximal wave of activation of the *Ilbp* gene (Fig. 3). At E18, scattered ILBP-positive columnar epithelial cells are evident overlaying nascent villi in the distal region of the small intestine (Fig. 4 *A*), as well as in the colonic epithelium. During the first postnatal week, ILBP production expands bidirectionally to involve additional columnar epithelial cells in the distal half of the ileum and in the cecum and colon (Fig. 3). By P7, clusters of ILBP-positive cells are interspersed among large areas of ILBP-negative cells in the proximal colon and cecum. These cells coexpress known markers of the enterocytic lineage such as I-FABP (data not shown). In the distal half of the ileum, most villus-associated enterocytes are ILBP positive. ILBP is not detectable in proliferating (BrdUrd-positive) cells located in the P2-P7 intervillus epithelium or in members of the goblet or enteroendocrine cell lineages (Fig. 4 *B* plus data not shown).

Just after P7, the expression domain of *Ilbp* abruptly "collapses," resulting in confinement of ILBP-positive, villus-associated enterocytes to the distal ileum. The extinction of *Ilbp* expression in the proximal colon and mid-ileum occurs during P7–P11 (Fig. 3). This is followed by a wave of reactivation that moves from the distal to proximal portions of the ileum over a 2-wk period. There are three characteristic cellular patterns of ILBP staining found at this stage of gut morphogenesis: (*a*) distal ileal villi contain a wholly ILBP-positive population of enterocytes (Figs. 3 and 4 *C*); (*b*) more proximal villi contain vertical coherent bands or stripes of wholly ILBP-positive enterocytes, each emanating from a given crypt and adjacent vertical coherent bands of wholly ILBP-negative stripes derived from adjacent crypts (Fig. 4, *D* and *E*); and (*c*) at the leading proximal portion of the gene's expression domain, villi generally contain a scattered population of ILBP-positive and ILBP-negative cells, giving them a speckled or mosaic appearance (Fig. 4 *F*). The distribution of wholly positive, striped, and speckled villi follows the wave of activation of *Ilbp* from P11 to P28; i.e., at any one point in time, the proximal portion of *Ilbp* expression domain contains striped villi while the leading edge consists of a predominant population of speckled villi composed of ILBP-positive and -negative cells with only a few striped and essentially no wholly positive villi (Fig. 3). The ILBP-positive cells encountered in the P11–P28 ileum were defined as enterocytes, based on their morphologic appearance and by their ability to support expression of a variety of well-characterized lineage-specific markers including I-FABP and L-FABP (data not shown).

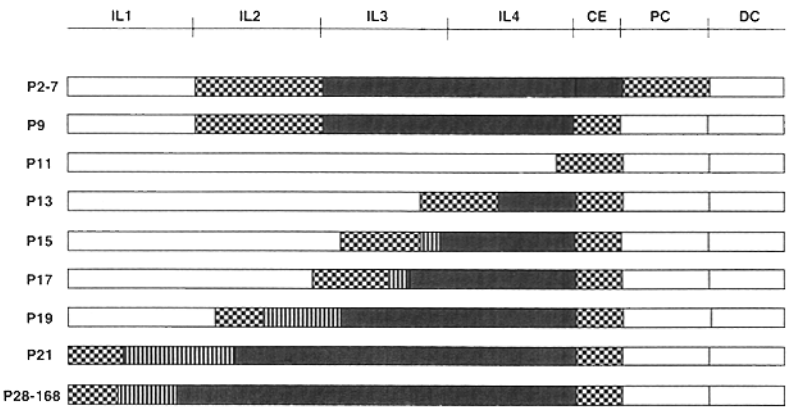


*Figure 3.* Summary of the distal-to-proximal wave of *Ilbp* activation in the developing FVB/N mouse intestine. The ileum has been operationally defined as the distal third of the small intestine. IL1 and IL4 refer to the proximal most (IL1) and distal most (IL4) quarters of the ileum. *CE*, cecum; *PC*, proximal colon; *DC*, distal colon. ▣ Segment containing scattered ILBP-positive epithelial cells; ▥, striped villi with vertical coherent bands of ILBP-positive enterocytes; ■, villi that contain ≥95% ILBP-positive enterocytes; □, ILBP not detectable in epithelial cells.

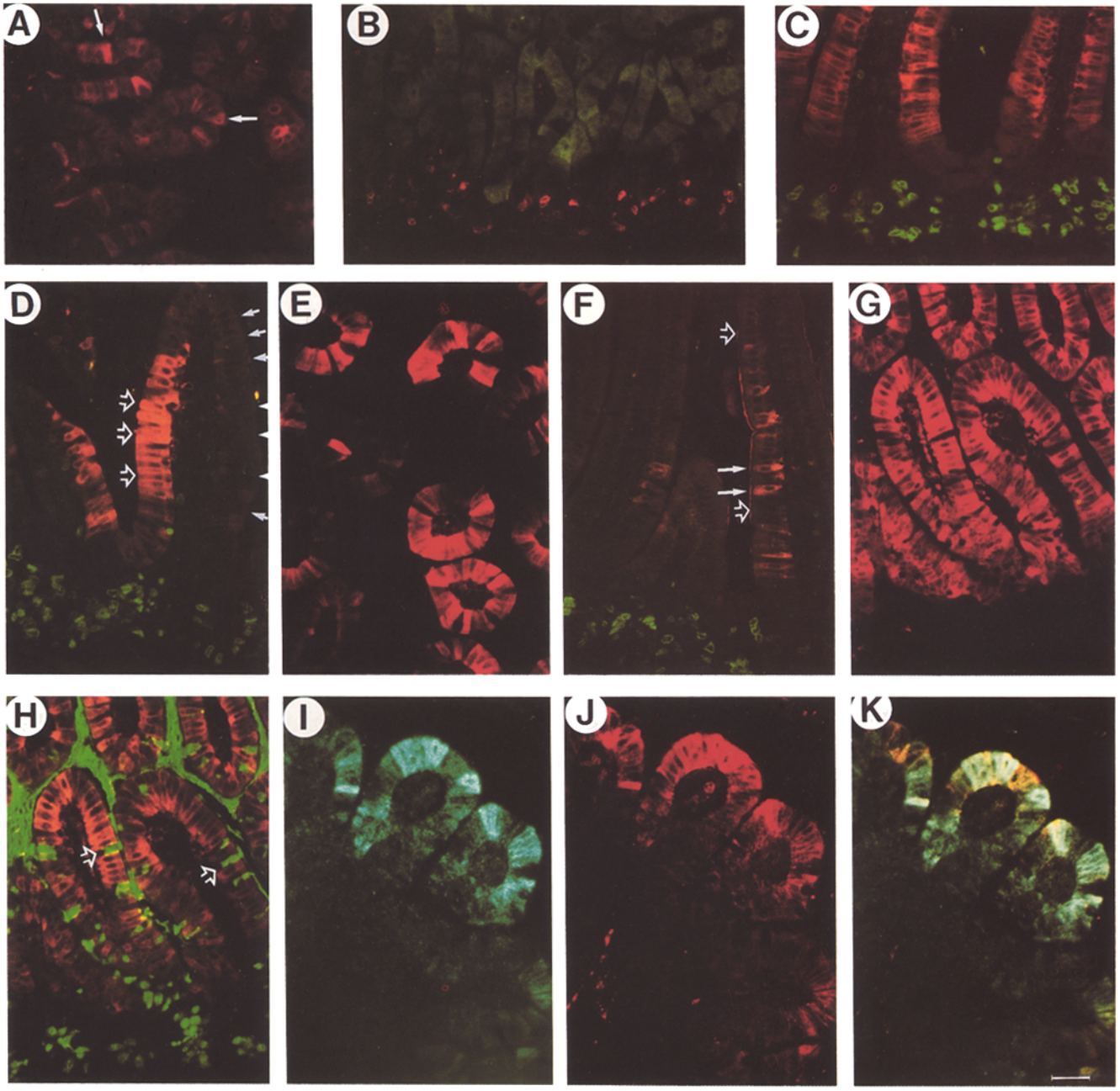


*Figure 4.* Immunocytochemical studies of the cellular patterns of ILBP expression in the developing FVB/N mouse intestine. (*A*) Cross-section of the distal small intestine of an E18 mouse, incubated with rabbit anti-ILBP followed by Texas red–labeled donkey anti–rabbit Ig. Scattered ILBP-positive columnar epithelial cells (*arrows*) are present on nascent villi. (*B*) Section prepared from P7 ileum incubated with rabbit anti-ILBP and goat anti-BrdUrd Ig. Antigen-antibody complexes were detected with goat anti-rabbit secondary antibody followed by gold-labeled secondary antibodies with silver enhancement and Texas red–labeled donkey anti–goat Ig. ILBP is confined to villus-associated enterocytes (*green-colored cells*) and is not detectable in proliferating BrdUrd-positive cells located in nascent crypts (*red-colored cells*). (*C–F*) Sections were incubated with goat anti-BrdUrd and rabbit anti-ILBP sera. Antigen-antibody complexes were then detected with fluorescein-labeled donkey anti–goat and Texas red–labeled donkey anti–rabbit sera, respectively. (*C*) ILBP is expressed in all villus-associated enterocytes located in the distal quarter of the ileum (IL4) of P28 FVB/N mice. (*D*) A villus located in the proximal quarter of the ileum (IL1) of this P28 mouse exhibits striping with a vertical coherent band of wholly ILBP-positive enterocytes (*open arrows*) located next to a vertical coherent band of wholly ILBP-negative enterocytes (*closed arrows*). (*E*) Coherent bands of ILBP-positive and -negative enterocytes are evident in cross-sections of villi located in the proximal quarter of the P28 ileum. (*F*) At the proximal-most border of *Ilbp*'s expression domain, villi contain a scattered population of ILBP-positive (*closed arrows*) and ILBP-negative enterocytes (*open arrows*). (*G*) Section prepared from the distal quarter of a P28 ileum stained with rabbit anti-ILBP and Texas red–labeled donkey anti–rabbit sera. (*H*) Double exposure of the same section shown in *G* after addition of FITC-conjugated UEA-I. Villus-associated UEA-I–positive goblet cells (*green*, *open arrows*) do not coexpress ILBP (seen as orange staining material in enterocytes). (*I*) Section prepared from the distal third of a P42 intestinal isograft incubated with rabbit anti-ILBP sera and immunogold-labeled goat anti–rabbit serum followed by silver enhancement. The section has been visualized using reflected light polarization microscopy. ILBP is present in villus-associated enterocytes (*aqua-colored cells*). (*J*) I-FABP detected in the same section as shown in *I*. Rabbit anti–I-FABP sera and Texas red–labeled donkey anti–rabbit Ig were used to identify immunoreactive cells (*red colored*). (*K*) Double exposure shows a population of enterocytes that coexpress both ILBP and I-FABP (*gray-green*) and a population of villus-associated enterocytes that only expresses I-FABP (*orange*). Bar, 25 μm.

By the conclusion of the weaning period (P28), the distal-to-proximal wave of *Ilbp* activation has completed its journey and the expression domain becomes fixed, remaining unchanged for at least the first 6 mo of postnatal life. ILBP is confined to enterocytes in the ileum and cecum. No immunoreactive protein can be detected in proliferating and nonproliferating crypt epithelial populations or in members of the Paneth cell, enteroendocrine, or goblet cell lineages (Fig. 4, *G* and *H* plus data not shown). Immunoreactive protein is not detectable in any epithelial cell population located in the proximal colon.

### *Intestinal Isografts Reveal that Establishment of Ilbp's Expression Domain Is Not Dependent on Exposure to Luminal Contents*

To assess the effect of luminal components on establishment and/or maintenance of *Ilbp*'s expression domain, E15 FVB/N small intestine and colon were implanted into the subcutaneous tissue of young adult male FVB/N recipients. After 6 wk, the isografts were removed and analyzed for the presence of ILBP using immunocytochemistry. The results demonstrate that the cell lineage–specific, differentiation-dependent, and regional patterns of *Ilbp* expression are not dependent on signaling pathways activated by exposure to pancreatic and biliary secretions, the microflora, or components of the diet such as mother's milk (Fig. 4, *I–K*).

### *Chimeric-Transgenic Mice Indicate That a Mosaic Pattern of ILBP Accumulation Can Occur in Enterocytes Derived from the Same Monoclonal Crypt*

The monophenotypic nature of villus striping (i.e., all enterocytes in a stripe are either ILBP-negative or ILBP-positive) suggests that members of this lineage are programmed within the monoclonal crypt, perhaps at the level of the stem cell or a committed progenitor, to either express or to not express *Ilbp* during their subsequent migration-associated differentiation program. In contrast, the presence of speckled villi containing isolated ILBP-positive enterocytes intermixed with ILBP-negative cells suggests a subtle heterogeneity in the differentiation program of enterocytes derived from the same monoclonal crypt or a heretofore unexpected degree of mixing of enterocytes from adjacent monoclonal crypts during their upward migration to the apical extrusion zone of ileal villi. If the latter were the case, we would also have to invoke a time-dependent change in this mixing because speckled villi are only evident at the leading edge of the proximally moving wave of *Ilbp* activation (Fig. 3).

We used chimeric-transgenic mice to determine whether the ILBP-positive and -negative enterocytes of a "speckled" villus are derived from the same monoclonal crypt. These mice are created by introducing D3 embryonic stem cells (129/Sv origin) stably transfected with *Fabp*/reporter DNAs into normal C57BL/6 blastocysts (29). The gut epithelium of the resulting chimeric animals will be composed of cellular populations derived from the stably transfected ES cell and cellular populations derived from the normal host blastocyst. A villus located at an ES/host cell border in the intestine of such a mouse can be composed of a discrete band of reporter-positive epithelial cells that emanate from a monoclonal, ES-derived crypt and an adjacent band of epithelial cells that do not produce the reporter encoded by the transgene because they emanate from a monoclonal, normal host blastocyst-derived crypt (Fig. 5 *A*). The 129/Sv ES- and C57BL/6 blastocyst-derived components of such a polyclonal villus can be differentiated from one another using the α-L-fucose–specific lectin, UEA-I. C57BL/6 enterocytes and enteroendocrine cells are UEA-I negative, while Paneth cells and a subset of goblet cells bind this lectin. In contrast, 129/Sv Paneth cells are UEA-I–negative, while villus-associated 129/Sv enterocytes, goblet cells, and a subset of enteroendocrine cells are UEA-I positive (17, 29). Studies in transgenic mice have shown that a fusion gene consisting of nucleotides −596 to +21 of rat *Fabpl* linked to the human growth hormone gene beginning at its nucleotide +3 (L-FABP$^{-596\ to\ +21}$/hGH$^{+3}$) is expressed throughout the duodenal-to-ileal axis, in all four gut epithelial cell lineages, as well as in proliferating and nonproliferating cells located in the lower and upper halves of small intestinal and colonic crypts (70, 75, 77). Adult C57BL/6←→D3(L-FABP$^{-596\ to\ +21}$/hGH$^{+3}$) chimeric-transgenic mice do not contain a mixture of hGH-positive and hGH-negative enterocytes within a given UEA-I–positive band of villus epithelial cells, providing independent support for the notion that each adult crypt is monoclonal (29). Moreover, the hGH and UEA-I phenotypes of villus-associated enterocytes are coincident, i.e., UEA-I-positive, ES-derived duodenal, jejunal, and ileal enterocytes are all hGH-positive, while a band of UEA-I–negative, blastocyst-derived enterocytes located on the same villus is wholly hGH-negative (29). With these findings in mind, sections prepared from the proximal ileum of 12-wk-old C57BL/6←→D3(L-FABP$^{-596\ to\ +21}$/hGH$^{+3}$) animals were stained with anti-ILBP and anti-hGH sera. The results reveal that a monoclonal ES-derived crypt can give rise to a band of hGH-positive enterocytes with a mixture of ILBP-positive and -negative phenotypes (Fig. 5, *B–D*).

An additional feature of chimeric-transgenic mice is that the band of host blastocyst-derived epithelium can serve as an internal control when assessing the biological effects of the transgene, i.e., the effect of a single gene product can be assessed in a single villus, located at a particular position along the cephalocaudal and crypt-to-villus axes, in a single animal. Immunocytochemical surveys of wholly ILBP-positive villi containing stripes of ES- and blastocyst-derived enterocytes revealed that cellular ILBP concentrations were the same in the adjacent stripes of hGH-negative and hGH-positive cells (data not shown). This finding established that hGH has no quantitative or qualitative effects on endogenous *Ilbp* gene expression, and that it would be "safe" to use hGH as a reporter for functional mapping studies of *Ilbp*'s promoter.

### *Mapping cis-Acting Elements that Regulate the Cell Lineage–specific, Axial, and Developmental Patterns of Ilbp Expression*

An initial assumption was made that the major determinants of *Ilbp*'s expression patterns were located in its 5′ nontranscribed region. A series of successive deletions of *Ilbp*'s 5′ nontranscribed domain were generated using a site selection strategy based solely on the availability of unique locations for cleavage by restriction endonucleases. Several pedigrees

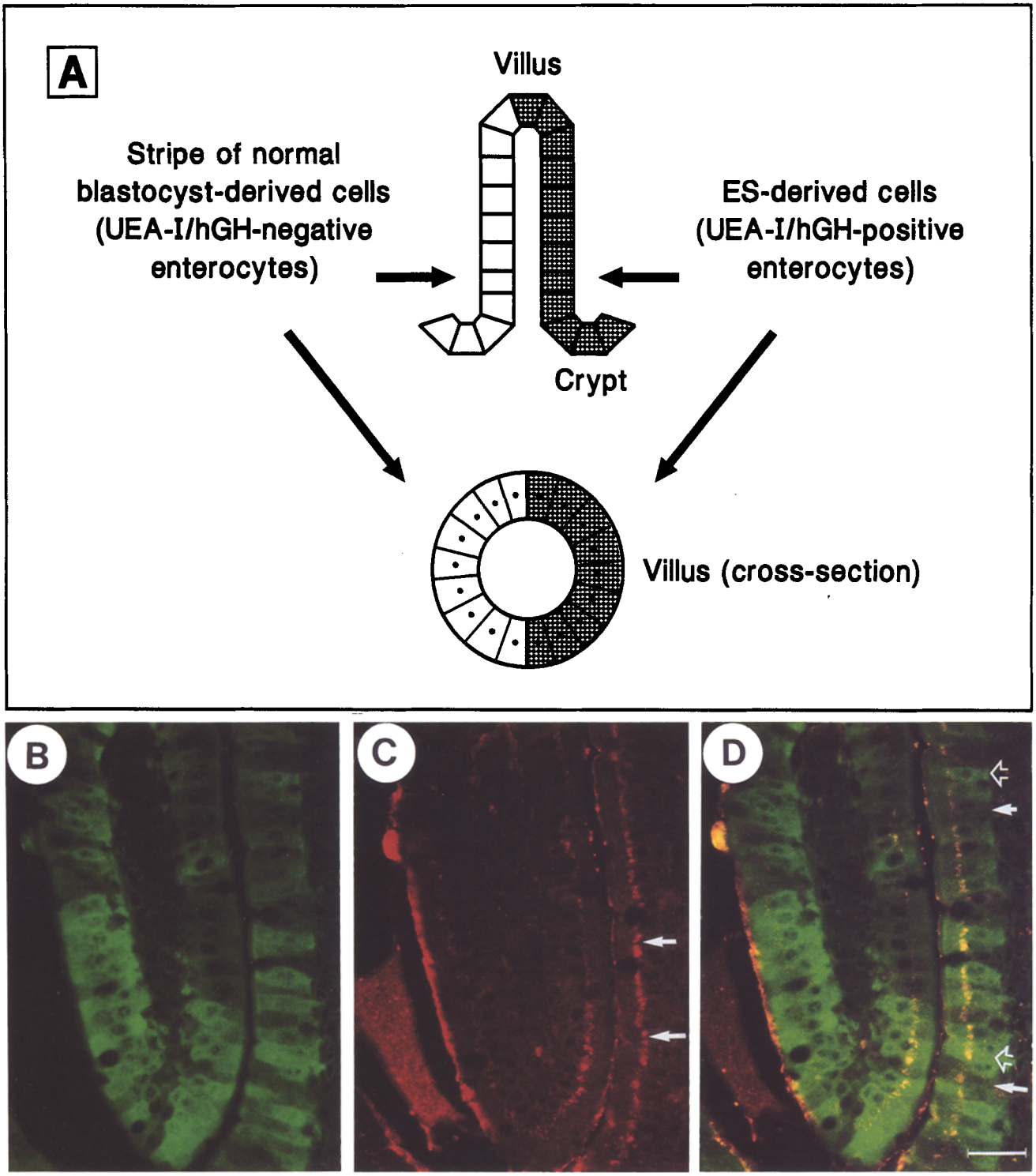


*Figure 5.* Multilabeling studies of 12-wk-old C57BL/6↔D3(L-FABP$^{-596\ to\ +21}$/hGH$^{+3}$) chimeric-transgenic mice reveal that enterocytes derived from a single monoclonal crypt can display marked variations in ILBP levels. (*A*) Schematic view of a villus located at the border of ES cell- and host-blastocyst-derived gut epithelium in an adult C57BL/6↔D3 chimeric mouse. The polyclonal villus receives contributions from a monoclonal ES-derived crypt, as well as from a monoclonal B6 crypt. (*B*) Cross-section of villi located in the proximal quarter of the ileum (IL1) of a 12-wk-old C57BL/6↔D3 (L-FABP$^{-596\ to\ +21}$/hGH$^{+3}$) mouse. The section is oriented similar to the cross section shown in *A*. Staining with rabbit anti-ILBP and fluorescein-labeled donkey anti-rabbit sera reveals ILBP-positive, villus-associated enterocytes as green-colored cells. (*C*) The same section as shown in *B*, incubated with goat anti-hGH followed by Texas red-labeled donkey anti-goat Ig. Golgi staining of hGH-positive enterocytes is evident (*arrows*). (*D*) A double exposure indicating that hGH-positive enterocytes derived from the same monoclonal ES crypt have both ILBP-positive (*open arrows*) and ILBP-negative phenotypes (*closed arrows*). Bar, 25 μm.

*Table I. Summary of Transgenic Mouse Pedigrees*

| Transgene | Liveborn mice screened | Founders* | Pedigrees expressing transgene‡ | Pedigree number | Transgene copy no./ haploid genome | [hGH]serum (ng/mL)§ |
|---|---|---|---|---|---|---|
| ILBP$^{-913\ to\ +48}$/hGH$^{+3}$ | 75 | 10 | 9 | 20 | 20 | 15–40 |
| | | | | 24 | ND | 0.5–1 |
| | | | | 52 | 27 | 9–150 |
| | | | | 56 | ND | 15–65 |
| | | | | 60 | ND | 21–120 |
| | | | | 66 | ND | 0.5–1 |
| | | | | 68 | 38 | 12–40 |
| | | | | 70 | ND | 2–4 |
| | | | | 71 | 8 | 33–44 |
| ILBP$^{-417\ to\ +48}$/hGH$^{+3}$ | 58 | 3 | 3 | 11 | 32 | 9–50 |
| | | | | 45 | 45 | 2–200 |
| | | | | 50 | 78 | 2–18 |
| ILBP$^{-145\ to\ +48}$/hGH$^{+3}$ | 64 | 5 | 3 | 3 | ND | <0.5 |
| | | | | 5 | ND | 1–4 |
| | | | | 17 | ND | <0.5 |
| | | | | 26 | ND | <0.5 |
| | | | | 60 | 94 | 16–60 |

* Founders were identified by PCR and Southern blot analyses of tail DNA.
‡ Expression was defined by radioimmunoassay of serum for hGH and by immunocytochemical surveys of tissue sections.
§ Serum was obtained by retroorbital phlebotomy from P28 F1 transgenic mice ($n$ = 2–4 mice/pedigree). Each serum sample was assayed in duplicate using a standard radioimmunoassay kit (Nichols Institute Diagnostic, San Juan Capistrano, CA). The range of the values recorded are shown. Note that the limit of sensitivity of the radioimmunoassay is 0.5 ng hGH/ml serum.

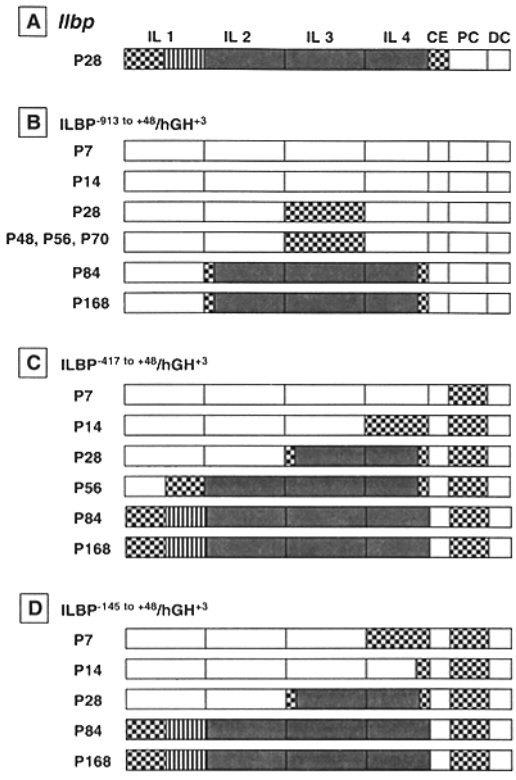


*Figure 6.* Summary of the spatial and temporal patterns of ILBP/hGH$^{+3}$ expression in 1–24-wk old transgenic mice. ▪ Segment contains scattered populations of hGH-positive epithelial cells; ▥, villi with vertical coherent bands of hGH-positive enterocytes; ■, villi with ⩾95% hGH-positive enterocytes; □, no detectable hGH expression in epithelial cells.

of FVB/N transgenic mice were generated, each containing nucleotides −913 to +48, −417 to +48, or −145 to +48 of *Ilbp* linked to hGH$^{+3}$ (Table I). The patterns of ILBP/hGH$^{+3}$ expression were compared and contrasted to the pattern of *Ilbp* expression at 1, 2, 4, 8–12, and 24 wk of age in transgenic mice and their age-matched, nontransgenic littermates using RNA blot hybridization and multilabel immunocytochemical techniques. The results are summarized in Fig. 6.

### *ILBP$^{-913\ to\ +48}$/hGH$^{+3}$*

This transgene is only expressed in the small intestine of adult members of the nine pedigrees of mice we surveyed. Moreover, none of the extraintestinal tissues examined in P7, P14, P28, and P168 animals belonging to the two lines studied in detail (Table I, 20 and 17) contained detectable levels of reporter mRNA or protein.

ILBP$^{-913\ to\ +48}$/hGH$^{+3}$ is silent in the duodenum, jejunum, ileum, cecum, and colon during the first 2 postnatal weeks. The transgene is first activated during the 4th postnatal week, well after the endogenous *Ilbp* gene (Fig. 6 *B*). Unlike *Ilbp*, initial activation occurs in the mid-portion of the ileum, where the hGH reporter is confined to villus-associated enterocytes. The pattern of transgene expression is speckled with hGH-positive and hGH-negative enterocytes distributed in a seemingly random pattern along the basilar-to-apical axis of the villus (Fig. 7 *A*). However, both hGH-positive and hGH-negative enterocytes contain similar levels of ILBP (Fig. 7, *B* and *C*). Between P70 and P84, the transgene's expression domain expands to include the distal three quarters of the ileum (Fig. 6 *B*). During this expansion, villi that formerly demonstrated a speckled pattern of reporter

production are "converted" to a monophenotypic pattern with wholly hGH-positive enterocytes. By the end of the 12th postnatal week, only wholly hGH-positive ileal villi are encountered (Fig. 7 *D*), with the exception of the very proximal and distal margins of ILBP$^{-913\ to\ +48}$/ hGH$^{+3}$'s expression domain (Fig. 6 *B*). The transgene shows appropriate differentiation-dependent activation, i.e., hGH (or ILBP) is not detectable in BrdUrd-positive or -negative crypt epithelial cells. Reporter production is not evident in the proximal quarter of the ileum, even in mice that are 24 wk old. Moreover, ILBP$^{-913\ to\ +48}$/hGH$^{+3}$ is silent in the cecum and colon from 1 to 24 wk of age (Fig. 6 *B*). The absence of expression in the colon is appropriate, at least from the 2nd postnatal week through adulthood. The absence of transgene expression in the cecal epithelium is inappropriate, contrasting with the persistent expression of *Ilbp* in this portion of the gut.

The delayed temporal pattern of ILBP$^{-913\ to\ +48}$/hGH$^{+3}$ activation in the ileum is also evident when measuring levels of reporter and ILBP mRNA. Between 4 and 12 wk of age, ILBP$^{-913\ to\ +48}$/hGH$^{+3}$ transgenic mice exhibit a sevenfold increase in their ileal hGH mRNA levels (from 18 $\pm$ 3 pg/$\mu$g total ileal RNA to 128 $\pm$ 17 pg/$\mu$g), while their ileal ILBP mRNA levels remain constant (Fig. 8).

### *ILBP$^{-417\ to\ +48}$/hGH$^{+3}$*

Like ILBP$^{-913\ to\ +48}$, this transgene is not expressed in any extraintestinal cell lineages, at least during the first 24 wk of life. Detailed developmental studies of two pedigrees of mice (Table I, lines 45 and 50) revealed that ILBP$^{-417\ to\ +48}$/ hGH$^{+3}$ is activated before ILBP$^{-913\ to\ +48}$/hGH$^{+3}$. At P7, the hGH reporter is only evident in the proximal colonic epithelium. There are two populations of hGH-positive cells in the colon: one belongs to the enterocytic lineage, based on its ability to produce ILBP and I-FABP, while the other can be assigned to the goblet cell lineage based on its reactivity with UEA-I (17) but not with anti-ILBP and I-FABP sera (data not shown).

By P14, reporter-positive epithelial cells are present in the proximal colonic enterocytes, goblet cells, and villi located in the distal quarter of the ileum (Fig. 6 *C*). Virtually all hGH-positive cells in the ileum coexpress ILBP and I-FABP (data not shown). In contrast, none of the hGH-positive cells react with UEA-I.

ILBP$^{-417\ to\ +48}$/hGH$^{+3}$'s expression domain moves proximally in the ileum between P14 and P28 (Fig. 6 *C*). By P28, villi containing wholly hGH-positive populations of enterocytes are distributed throughout the distal half of the ileum. hGH shows an appropriate pattern of differentiation-dependent activation in enterocytes as they migrate along the crypt-to-villus axis (Fig. 7 *E*). At P56, transgene expression has extended to the junction between the proximal two quarters of the ileum (Fig. 6 *C*). By 12 wk (P84), the pattern of transgene expression is largely equivalent to that of *Ilbp* (Fig. 6, *A* and *C*). The distal three quarters of the ileum (IL2–IL4) contain wholly reporter-positive villi. The proximal quarter of the ileum (IL1) contains striped villi plus speckled villi (Figs. 6 *C* and 7 *F*). At the leading (i.e., most proximal) edge of ILBP$^{-417\ to\ +48}$'s expression domain, only a subset of the scattered hGH-positive enterocytes coexpress ILBP, and only a subset of the scattered ILBP-positive enterocytes produce hGH (data not shown). The delayed temporal pattern of ILBP$^{-417\ to\ +48}$/hGH$^{+3}$ activation in the ileum (compared to *Ilbp*) is reflected by a marked increase in steady-state levels of hGH but not ILBP mRNA between the 4th and 12th postnatal weeks (Fig. 8).

Unlike *Ilbp*, ILBP$^{-417\ to\ +48}$/hGH$^{+3}$ remains silent in the cecum from the first through at least the 24th postnatal week and persists in proximal colonic enterocytes (Fig. 7 *G*). The hGH-positive population of colonic goblet cells is no longer evident by P28.

### *ILBP$^{-145\ to\ +48}$/hGH$^{+3}$*

Only one out of five pedigrees containing this transgene produced detectable levels of reporter mRNA or protein in the intestine (Table I, line 60). Two of the other lines (lines 17 and 26) did not express ILBP$^{-145\ to\ +48}$/hGH$^{+3}$ in their gastrointestinal tracts or in any of the extraintestinal tissues surveyed. By 4 wk of age, members of pedigree 3 contained low levels of hGH mRNA in the kidney, but not in the stomach, small intestine, colon, or other tissues (data not shown). hGH mRNA was confined to the adrenal in 4-wk-old members of pedigree 5. Both of these patterns of transgene expression are anomalous: kidney and adrenal RNA do not contain detectable levels of ILBP mRNA in these transgenic mice or in their normal littermates (data not shown).

Analysis of pedigree 60 revealed that by P7, ILBP$^{-145\ to\ +48}$ is activated in scattered villus-associated, UEA-I–positive goblet cells located in the distal quarter of the ileum and in the proximal colonic epithelium (Figs. 6 *D*, 7 *H–J*, and 9 *A–D*). ILBP$^{-145\ to\ +48}$/hGH$^{+3}$ is the only transgene among the three analyzed that exhibits an extinction of expression in the ileum between the 1st and 2nd wk of postnatal life. This extinction mirrors the silencing of *Ilbp* expression except that it involves members of the goblet cell rather than enterocytic lineage. By P14, only a small segment of the distal quarter of the ileum (IL4) contains villus-associated hGH-positive cells (Fig. 6 *D*). Most of these cells appear to be enterocytes, i.e. they are ILBP positive and I-FABP positive but UEA-I negative (data not shown). The expression domain of ILBP$^{-145\ to\ +48}$/hGH$^{+3}$ then expands between P14 and P28, traveling in a distal-to-proximal wave at a rate that is slower than that of *Ilbp*. For example, by P28, hGH is still limited to villi located in the distal half of the ileum (IL3 and IL4), whereas *Ilbp* expression extends to villi in IL1 (compare Figs. 3 and 6, *A* and *D*). At 4 wk of age, ILBP$^{-145\ to\ +48}$/hGH$^{+3}$ is expressed in virtually all villus-associated enterocytes in IL3 and IL4 (Fig. 7, *K* and *L*). Proliferating cells in the crypts and goblet cells do not contain detectable levels of the hGH reporter. A speckled cellular pattern of hGH staining is limited to the very proximal and distal edges of the transgene's expression domain. The proximal wave of ILBP$^{-145\ to\ +48}$/ hGH$^{+3}$ activation continues to move slowly so that by the 12th postnatal week, IL2-IL4 are composed of villi with wholly hGH- (and ILBP-) positive enterocytes. At 12 and 24 wk, IL1 contains villi with a speckled pattern of reporter production in their enterocytes.

ILBP$^{-145\ to\ +48}$/hGH$^{+3}$ expression in UEA-I-positive goblet cells is extinguished between P7 and P14 in the colon, just as it is in the distal ileum. However, by P14 and for at least the next 12–24 wk, expression of the transgene persists in colonic (but not cecal) enterocytes. These hGH-positive cells are clustered at the surface epithelial cuffs that surround the orifice of crypts (i.e., the colonic homologues of villi). Scat-

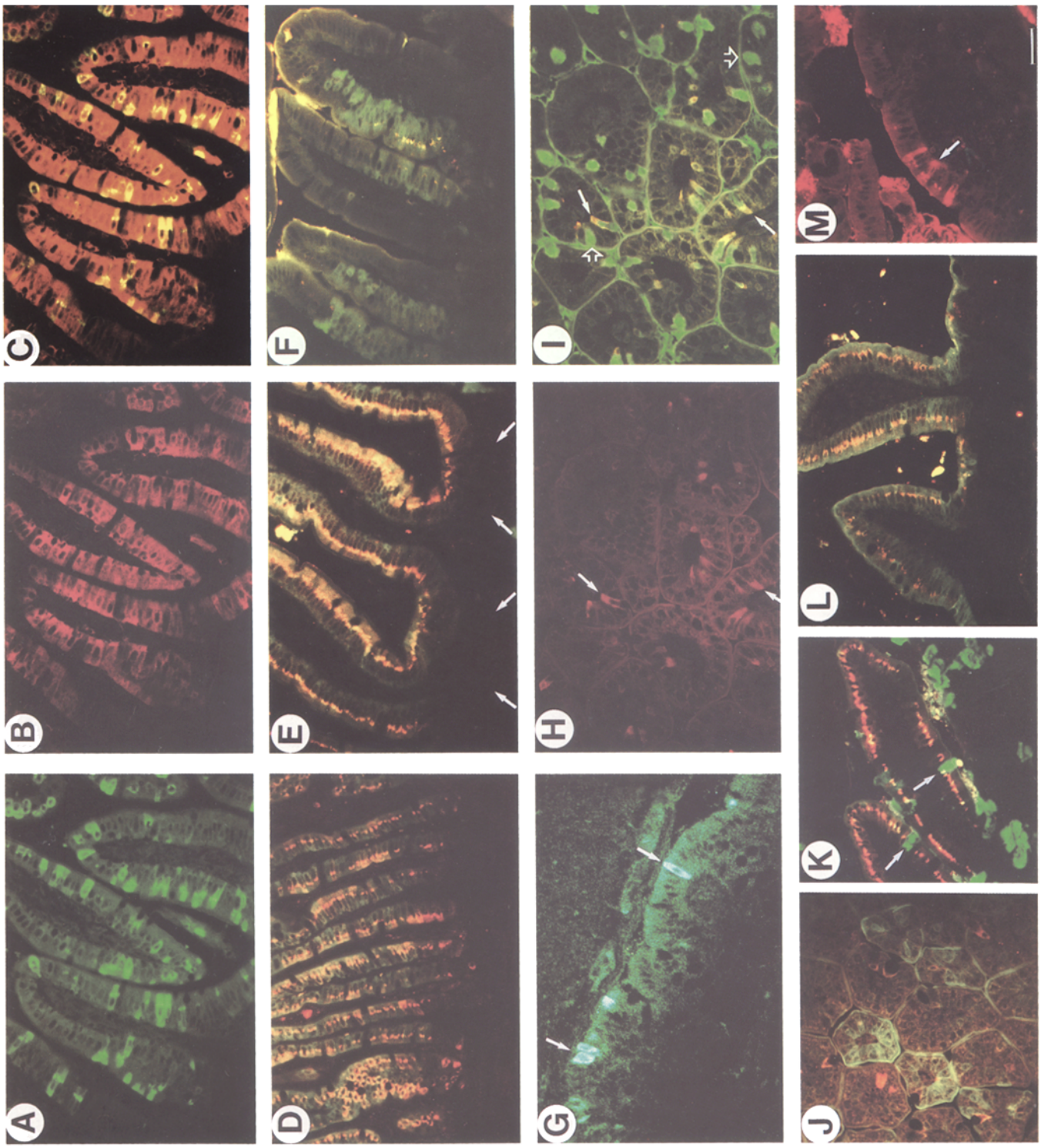


*Figure 7.* Immunocytochemical studies of the cellular patterns of ILBP/hGH$^{+3}$ expression during and after gut morphogenesis. (*A–C*) A section of ileum (IL3) recovered from a P28 ILBP$^{-913\ to\ +48}$/hGH$^{+3}$ transgenic mouse was incubated with goat anti-hGH and rabbit anti-ILBP sera. Antigen-antibody complexes were detected with fluorescein-labeled donkey anti–goat and Texas red–labeled donkey anti–rabbit secondary antibodies, respectively. (*A*) Villi are composed of a scattered population of hGH-positive and hGH-negative enterocytes. (*B*) The same section shows the homogeneous pattern of ILBP expression in villus-associated enterocytes. (*C*) Double exposure demonstrates that the hGH-positive enterocytes coexpress ILBP (*yellow cells*). (*D*) A section prepared from IL3 of a P84 ILBP$^{-913\ to\ +48}$/hGH$^{+3}$ mouse was incubated with goat anti-hGH and rabbit anti-ILBP sera. Antigen-antibody complexes were detected with CY3-labeled donkey anti–goat and fluorescein-labeled donkey anti–rabbit secondary Igs. The villi contain a wholly hGH-positive population of enterocytes (orange staining supranuclear Golgi apparatus) that coexpress ILBP (*green staining material in cytoplasm*). (*E*) Section from IL3 of a P28 ILBP$^{-417\ to\ +48}$/hGH$^{+3}$ mouse stained as in *D*. A homogeneous pattern of hGH expression (*orange*) is evident in all villus-associated ILBP-positive (*green*) enterocytes located in this portion of the ileum. The arrows point to the crypt region. (*F*) Villi from the proximal ileum

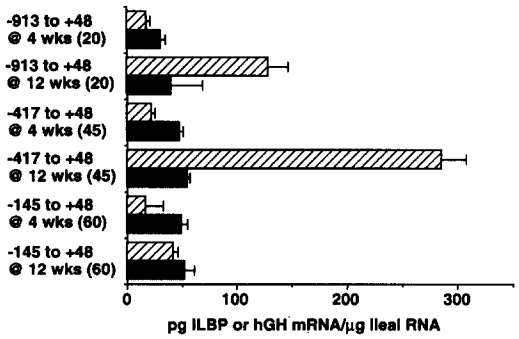


*Figure 8.* Analysis of steady-state levels of ILBP and hGH mRNAs in the ileum of 4- and 12-wk-old ILBP/hGH$^{+3}$ transgenic mice. mRNA concentrations were determined as described in Materials and Methods. The pedigrees used for these analyses are indicated in parenthesis. $n$ = 2 mice/time point. The mean value ± 1 SD has been plotted. ▨, hGH; ■, ILBP.

tered reporter-positive cuffs are evident. These occur singly or in small patches (Fig. 7 *M*). Moreover, a given surface epithelial cuff can contain either a wholly positive population of hGH-positive cells (the colonic equivalent of a wholly reporter-positive villus?), a cluster of hGH-positive cells that extend over a segment of the hexagonal shaped cuff (the equivalent of a striped villus?), or some scattered reporter-positive cells dispersed between reporter-negative cells (the equivalent of a speckled villus?).

### *The Presence of Multiple Copies of Each ILBP/hGH$^{+3}$ Transgene has no Detectable Effects on the Patterns of Ilbp Expression*

94 copies of ILBP$^{-145\ to\ +48}$/hGH$^{+3}$/haploid genome has no detectable quantitative or qualitative effects on *Ilbp* expression: (*a*) the steady-state level of ILBP mRNA in the ileum of 4–12 wk-old transgenic mice is equivalent to that documented in nontransgenic FVB/N mice (~50 pg/μg total cellular RNA; see Figs. 2 and 8); and (*b*) the expression domain of *Ilbp* is indistinguishable in ILBP$^{-145\ to\ +48}$/hGH$^{+3}$ mice and their age-matched littermates. This lack of an effect of the transgene on *Ilbp* expression is also true in mice containing ILBP$^{-913\ to\ +48}$/hGH$^{+3}$ or ILBP$^{-417\ to\ +48}$/hGH$^{+3}$, and it is compatible with our finding that hGH has no effect on *Ilbp* accumulation in C57BL/6↔D3(L-FABP$^{-596\ to\ +21}$/hGH$^{+3}$) mice.

## *Discussion*

### *A Functional Map of Ilbp's Promoter*

Fig. 10 summarizes the results of our functional mapping studies of *Ilbp*'s 5′ nontranscribed domain. A remarkably compact region of the gene that spans nucleotides −145 to +48 contains *cis*-acting elements sufficient to produce an appropriately directed distal-to-proximal wave of activation in the ileum and to subsequently correctly confine reporter production to villus-associated ileal enterocytes. In addition, these sequences can establish and maintain an appropriate axial distribution of wholly reporter-positive villi in the distal three quarters of the ileum, as well as striped and speckled villi in the proximal portion of *Ilbp*'s expression domain. Nucleotides −145 to +48 are unable to reproduce four features of *Ilbp* expression: (*a*) the normal postnatal extinction of (reporter) expression in the colon is not evident; (*b*) cecal expression is never detectable; (*c*) the distal-to-proximal wave of ILBP$^{-145\ to\ +28}$ reactivation during P7 to P28 moves more slowly than the wave of activation of the intact endogenous *Ilbp* gene; and (*d*) expression during the first 2 wk of postnatal life in the ileum and proximal colon occurs in goblet cells rather than being confined to enterocytes. However, additional pedigrees of mice containing ILBP$^{-145\ to\ +48}$/hGH$^{+3}$ are needed to evaluate the significance of these differences. Nucleotides −417 to −146 appear to contain a "temporal" suppressor of ileal expression that delays initial activation of the gene until the 2nd postnatal week. Nucleotides −913 to −418 have three types of suppressors: (*a*) a temporal suppressor that further delays initial activation of the gene until the 3rd to 4th postnatal week, but does not appear to modify the rate of movement of *Ilbp*'s expression domain from IL4 to IL2; (*b*) a spatial suppressor that prohibits gene expression in the proximal quarter of the ileum and in the proximal colon; and (*c*) a cell lineage suppressor that pro-

(IL1) of the same animal as shown in *E* exhibit a striped pattern of hGH (*orange*) and ILBP (*green*) expression. (*G*) The proximal colon from the P28 ILBP$^{-417\ to\ +48}$/hGH$^{+3}$ mouse contains scattered populations of hGH-positive enterocytes (*arrows*) that have been detected with goat anti-hGH followed by immunogold-labeled rabbit anti-goat and silver enhancement technique. (*H* and *I*) Section of distal ileum (IL4) from a P7 ILBP$^{-145\ to\ +48}$/hGH$^{+3}$ mouse incubated with goat anti-hGH sera and fluorescein-labeled UEA-I. Antigen-antibody complexes were detected with CY3-labeled donkey anti-goat Ig. (*H*) Scattered hGH-positive epithelial cells are present on distal ileal villi (*arrows*). (*I*) Dual exposure demonstrating that hGH is expressed in a subset of UEA-I-positive goblet cells (*closed arrows*). Note that many UEA-I-positive goblet cells do not contain detectable levels of the hGH reporter (*open arrows*). (*J*) Section prepared from the distal ileum of the same animal as shown in *H* and *I* incubated with goat anti-hGH and rabbit anti-ILBP sera. Antigen–antibody complexes were detected with CY3-labeled donkey anti-goat and FITC-labeled donkey anti-rabbit sera. Dual exposure shows a scattered population of hGH-positive goblet cells (*red*) that is distinct from villus-associated ILBP-positive enterocytes (*green*). (*K*) Sections prepared from the ileum (IL3) of a P28 ILBP$^{-145\ to\ +48}$/hGH$^{+3}$ mouse, stained using the reagents described for *H* and *I*. hGH expression (*orange-red*) has been extinguished from villus-associated goblet cells (*green*, *arrows*) by this point in development. (*L*) Sections of IL3 from the same P28 mouse as shown in *K* stained using the reagents described in *D*. All villus-associated enterocytes located in this portion of the ileum at this stage of development coexpress hGH and ILBP. (*M*) ILBP$^{-145\ to\ +48}$/hGH$^{+3}$ expression persists in enterocytes located in the surface epithelial cuffs (*arrows*) of the proximal colon from a P84 mouse. The section was incubated with goat anti-hGH followed by the CY3-labeled donkey anti-goat secondary antibody. Bar, 25 μm.

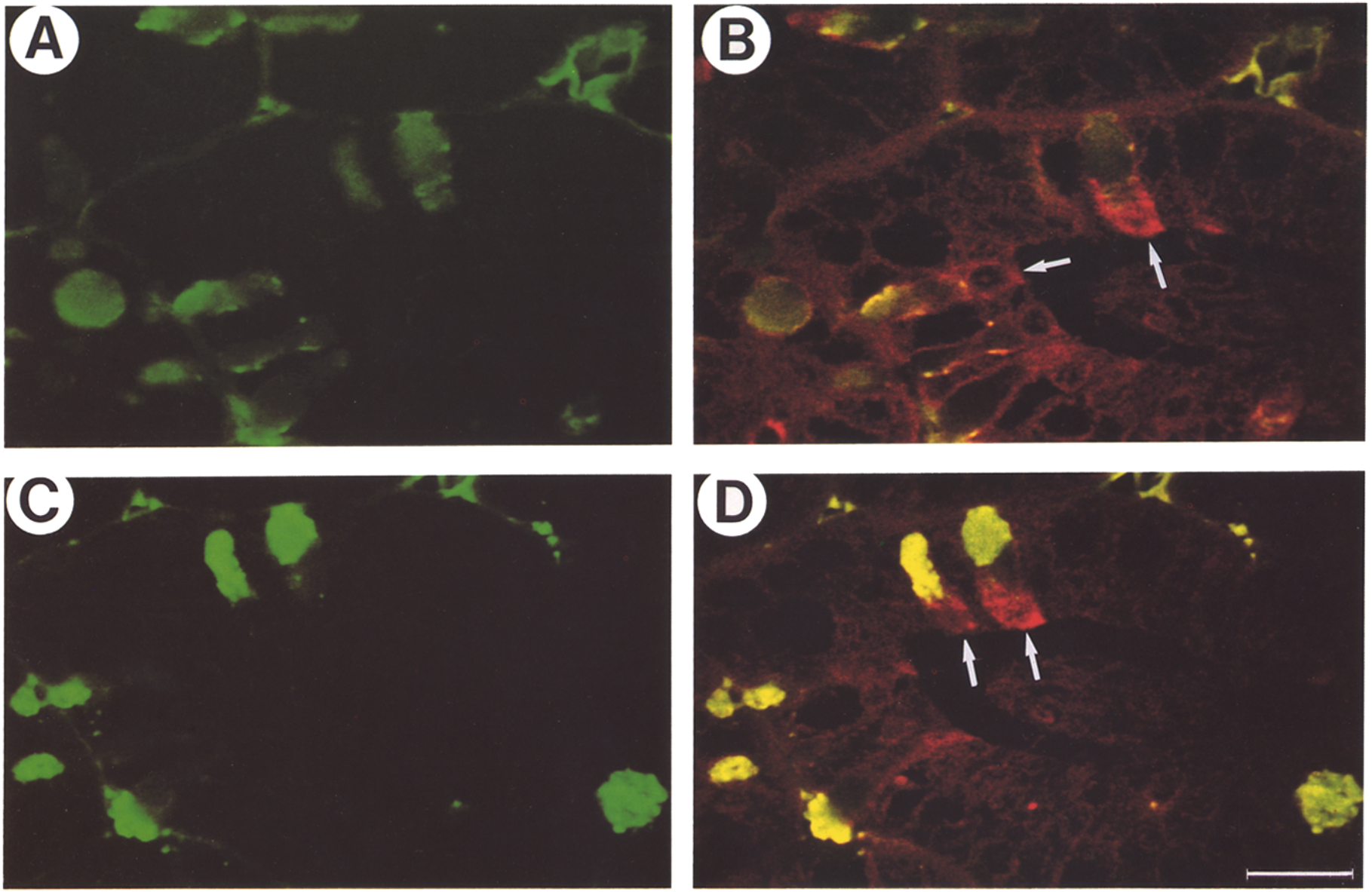


*Figure 9.* Confocal microscopy of villi located in the distal quarter of the ileum of a P7 ILBP$^{-145\ to\ +48}$/hGH$^{+3}$ mouse. The same villus is viewed in all four panels. *A* and *B* are on the same focal plane, and they are separated by 2 μm from the focal plane of *C* and *D*. Sections were incubated with fluorescein-labeled UEA-I and goat anti-hGH followed by detection with Texas red–labeled donkey anti–goat secondary Ig. *A* and *C* show the UEA-I staining pattern of villus-associated goblet cells. *B* and *D* are a double exposure and reveal that a subset of UEA-I–positive goblet cells coexpress hGH (*arrows*). Bar, 25 μm.

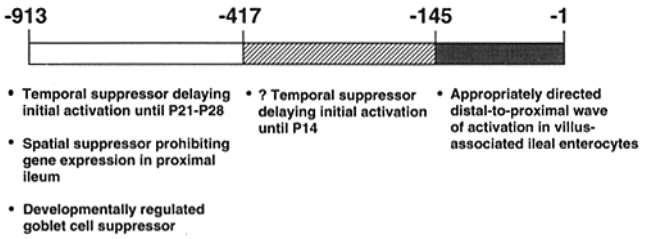


*Figure 10.* A functional map of the 5′ nontranscribed domain of mouse *Ilbp*. A question mark has been placed next to the proposed temporal suppressor between nucleotides −417 to −146 because its existence was inferred from an analysis of members of only one pedigree of ILBP$^{-145\ to\ +48}$/hGH$^{+3}$ mice.

hibits expression in goblet cells during the first 2 postnatal weeks.

### *Sequence Comparison of Functionally Defined Regions of Homologous and Nonhomologous Genes Expressed in Ileal Villus-associated Enterocytes*

Promoter mapping studies of *Ilbp*, *Fabpi*, and *Fabpl* conducted in transgenic mice indicate that their duodenal-to-ileal gradients of expression in villus-associated enterocytes can be established and maintained by remarkably compact sequences located within 103 bp (*Fabpi*), 132 bp (*Fabpl*), and 145 bp (*Ilbp*) of their start sites of transcription (references 12, 70; Fig. 10). Nucleotides −103 to +28 of rat *Fabpi*, like nucleotides −145 to +48 of *Ilbp*, are sufficient to restrict production of hGH to the enterocytic lineage in adult mice. This region contains one copy of a repeated 14-bp element that is conserved in the orthologous mouse and human genes (24, 73). Cotransfection studies in established epithelial cell lines indicate that hepatic nuclear factor-4 (HNF-4) and apolipoprotein regulatory protein-1, two members of the steroid hormone receptor superfamily of transcription factors that are produced in enterocytes, bind to this element and can activate I-FABP$^{-103\ to\ +28}$/hGH$^{+3}$ (61). Nucleotides −277 to −184 of *Fabpi* contains *cis*-acting suppressors of hGH expression in the ileum and proximal colon, and they include a 24-bp element spanning nucleotides −212 to −188 that binds nuclear factors present in colonic but not small intestinal epithelial cells (12). In contrast, nucleotides −1178 to +278 of *Fabpi* contain sequences that enhance ileal and colonic expression (12). We were unable to detect any similarities between nucleotides −913 to +48 of *Ilbp* and these functionally defined portions of *Fabpi* using dot matrix comparisons. These analyses also failed to disclose any obvious sequence similarities between ILBP$^{-913\ to\ +48}$ and nucleotides −3424 to +54 of the nonhomologous human sucrase isomaltase gene, which confine hGH expression to distal jejunal and ileal villus-associated enterocytes in adult transgenic mice (44). The functionally mapped portions of the *Ilbp* do contain matches to consensus binding sequences for a number of known transcription factors (compare Fig. 1 *C* and 10). Several of these sites are also predicted to occur in the *Fabpi* promoter (e.g., C/EBP, HNF-4, HNF-5, ANTP; see reference 12). However, the relevance and significance of these predictions are unknown at present. Higher resolution functional maps of the *Ilbp* and *Fabpi* promoters are needed, as are analyses of the cell lineage-specific, axial, and temporal patterns of expression of these transcriptional factors in the gut epithelium (4).

### *The Evolution of Ilbp's Expression Domain Occurs during a Critical Period in Gut Morphogenesis*

***Axial Patterning.*** *Ilbp* represents the only enterocytic-specific gene that we know of that has a distal-to-proximal wave of activation. The timing of this activation makes *Ilbp* a very attractive molecular marker of the intestine's axial patterning. Axial patterning appears to be expressed at different times and in different directions during intestinal development. As noted above, the initial cytodifferentiation of the intestinal endoderm to an epithelial monolayer proceeds in a proximal-to-distal wave during late gestation. *Fabpi* and *Fabpl* follow this wave during their activation in the duodenum, jejunum, and ileum. Establishment of *Ilbp*'s expression domain occurs during postnatal life and proceeds in the opposite direction. The patterns of activation of other ileal-specific genes (81) need to be examined to determine whether this distal-to-proximal wave of differentiation is a general feature, or whether the ileum and other segments of the gut are capable of establishing their positional addresses through a bidirectional flow of information along the cephalocaudal axis.

The source of the information that directs *Ilbp*'s regional patterns of activation remains unclear. The isograft experiments reported in this work suggest that the E15 intestine has sufficient information to direct establishment and maintenance of *Ilbp*'s expression domain without instruction from luminal contents. However, these experiments do not answer the question of whether axial patterning reflects a cell autonomous process encoded entirely within the E15 endoderm, or whether it is programed through instructive/permissive interactions between the mesoderm and endoderm with initial patterning occurring in the mesoderm (as is the case with the midgut of *Drosophila* larvae; see references 31, 33, 50, 55, 76). Insights about the contribution of the mesoderm to axial patterning could be obtained by implanting recombinant xenografts, composed of endoderm derived from one region of E14/E15 mouse intestine and mesoderm derived from the same or other portions of its cephalocaudal axis, into the subcutaneous tissues or kidney capsules of young adult syngenic recipients (35). A gene such as *Ilbp* should be a useful marker of regional identity in these types of experiments.

***Homogeneous, Striped, and Speckled Villi.*** The mechanisms responsible for converting the enterocytic patterns of *Ilbp* and ILBP/hGH$^{+3}$ expression in ileal villi from wholly negative to speckled/striped to wholly positive are unknown. Nonetheless, this phenomenon should be viewed in light of developmental changes in the migration/replacement rates of enterocytes and current hypotheses about the nature of the crypt's stem cell hierarchy.

[$^3$H]Thymidine-labeling studies indicate that proliferating cells located in the intervillus epithelium of E17 mouse ileum do not complete their migration up and subsequent extrusion from villi until P14 (3). Thus, the initial cycle of activation and extinction of *Ilbp* expression in E18–P11 enterocytes occurs during a period that coincides with their "birth" in late fetal life and completion of their "death" (exfoliation) during the 2nd postnatal week. Cellular proliferation and migration rates increase between the suckling and weaning periods,

reaching a rough equilibrium state by P28. This equilibrium is achieved at the completion of a period of rapid crypt multiplication, changing crypt-to-villus ratios, and villus lengthening (1, 9). We have not measured the rate of enterocytic replacement at specific positions along the cephalocaudal axis of the ileum during P14–P28. We have determined that as the distal-to-proximal wave of *Ilbp* (re)activation from P11 to P28 passes through a particular point along IL4→IL1, the cellular pattern of *Ilbp* expression in a villus is converted from wholly negative to speckled/striped to wholly positive during a period of ~4 d (Fig. 3). Although we do not know whether the rate of conversion of *Ilbp* expression patterns is more rapid, equivalent, or slower than the transit time of enterocytes on P13–P28 ileal villi, it is clear that evolution of the pattern of transgene expression can span a period of 70–84 d (i.e., ILBP$^{-913\ to\ +48}$/hGH$^{+3}$; Fig. 6 *B*). Such a slow rate of change takes place over many generations of enterocytes; the ileal villus transit time in adult mice is only 29–35 h (82). This raises a question about whether these slowly evolving changes reflect an alteration in the properties (programming) of an existing population of active crypt stem cells, or whether it signifies a replacement of these stem cells through recruitment of other potential stem cells.

There are two current views of crypt stem cell organization in adult mice (summarized in reference 41). One view, known as the stem cell pedigree concept, postulates that a single, slowly dividing "master" stem cell ultimately maintains the epithelial cell population of each crypt with the help of descendants termed transit or temporary stem cells, i.e., active stem cells are arranged in a pedigree with the most slowly cycling master stem cell at the apex of this pedigree (41, 46). Mutational assays suggest that some of these temporary stem cells may maintain themselves for ≤12 wk in the small intestine (78, 79). In the other view, the adult mouse intestinal crypt contains several functionally equivalent, self-maintaining stem cells which, in turn, arise from a single stem cell during gut morphogenesis (39–41, 53). Our studies with adult chimeric-transgenic mice indicate that a given monoclonal crypt is capable of giving rise to a population of enterocytes with a mixture of ILBP phenotypes (i.e., the speckled villi at the proximal boundary of the gene's expression domain). If these cells are derived from multiple active stem cells in a crypt, it would appear that *Ilbp* and ILBP/hGH$^{+3}$ transgenes are reporting subtle differences in the regulatory environments of their descendants (and perhaps the stem cells themselves) both during and after completion of crypt morphogenesis/purification. The other view, i.e., that the decision to express ILBP (or hGH) is not programmed at the level of the stem cell or its immediate descendants, but rather arises from permissive/instructive interactions between villus-associated enterocytes and the underlying mesenchyme during cellular translocation along the crypt-to-villus axis, would imply a remarkable heterogeneity in the character of this mesenchyme.

Although the cellular and molecular mechanisms responsible for maintaining speckled and striped cellular patterns of ILBP and hGH production in the mouse intestine are not known, the pattern appears to be related to the location of the boundaries of the genes' expression domains. This is also true for *Fabpl* and L-FABP/hGH$^{+3}$ transgenes (70). Adult male and female adult transgenic mice containing one of five different L-FABP/hGH$^{+3}$ fusion genes, each with successively smaller segments of *Fabpl*'s 5′ nontranscribed domain, exhibit a striped pattern of reporter expression in small intestinal villi (58, 70). The frequency of striped villi at a given location along the duodenal-to-ileal axis increases as more of the 5′ nontranscribed domain of rat *Fabpl* is removed, e.g., ~10% of duodenal villi have hGH-negative stripes in adult L-FABP$^{-596\ to\ +21}$/hGH$^{+3}$ mice compared to 50% in L-FABP$^{-132\ to\ +21}$/hGH$^{+3}$ animals. Although the endogenous mouse *Fabpl* gene shows no evidence of striping in the duodenal and jejunal villi of transgenic mice or their normal littermates, ileal villi located at the distal boundary of its expression domain contain vertical coherent stripes of enterocytes with distinct levels of immunoreactive L-FABP. The proximal-most position where hGH striping first appears seems to coincide with the distribution of hGH mRNA levels, i.e., when the "volume" of transgene expression is lowered below a threshold level in the distal intestine, striping inevitably appears (70). These observations indicate that the capacity to express a striped pattern of reporter expression is not limited to ileal villi. Moreover, this capacity persists throughout adulthood and may provide a marker of variations in the biological properties of stem cells or their immediate descendants that populate different "monoclonal" crypts supplying the same villus.

***Temporal Suppressor Elements in Ilbp.*** The temporal patterns of *Ilbp* activation appear to be modulated by a series of *cis*-acting suppressors. Removal of these temporal suppressor elements allows ILBP$^{-145\ to\ +48}$/hGH$^{+3}$ expression to be initiated at a stage of development that is similar to that of the endogenous gene. However, the distal-to-proximal evolution of the transgene's expression domain is still slower than that of *Ilbp*. *Ilbp* contains a predicted glucocorticoid response element in intron I (5′-CAAACACTCTGTTCT-3′; see Fig. 1 *B*). An increase in circulating glucocorticoid levels occurs at the suckling/weaning transition and mediates a number of changes in the enterocyte's differentiation program (28, 43). This increase coincides with the time of (re)activation of *Ilbp* and subsequent rapid expansion of its expression domain. Although the hGH gene contains a GRE in its first intron (48), it may not be functionally equivalent to the GRE in the first intron of *Ilbp*, thereby accounting for the delay in axial expansion of the transgene's expression domains. Characterization of the functional role of the GRE in *Ilbp* plus further mapping of the *cis*-acting temporal suppressors located between nucleotides −913 and −146 should provide insights about the molecular mechanisms that regulate gene transcription during and after completion of gut morphogenesis.

***Ilbp's Developmentally Regulated Goblet Cell Suppressor.*** The goblet cell–specific suppressor located between nucleotides −913 and −418 is remarkable for at least two reasons: (*a*) its function is only revealed during the first 2 wk of postnatal life; and (*b*) its existence provides additional evidence in support of the notion that enterocytes and goblet cells are derived from a common transit cell (51). The identification of a developmental stage-specific goblet cell specific suppressor in *Ilbp* provides an opportunity to study the differentiation of these lineages at different stages of gut morphogenesis.

We are grateful to David O'Donnell for his participation in the generation and maintenance of transgenic mice, Michelle Hermiston for providing

chimeric-transgenic animals, Per Falk for his help with intestinal isografts and lectin-staining protocols, Rob Murphy for preparing some of the RNA samples used in this study, plus Kevin Roth, Bill Colemen, and Elvie Taylor for their suggestions and technical assistance with the immunocytochemical analyses. We thank Ann Stone for her assistance in preparing this manuscript.

This work was supported by a grant from the National Institutes of Health (DK37960).

Received for publication 4 May 1994 and in revised form 22 June 1994.

## *References*

1. Al-Nafussi, A. I., and N. A. Wright. 1982. Cell kinetics in the mouse small intestine during immediate postnatal life. *Virchows. Arch. Cell Pathol.* 40:51–62.
2. Bradley, A. 1987. *In* Production and Analysis of Chimaeric Mice in Teratocarcinoma and Embryonic Stem Cells: A Practical Approach. E. J. Robertson, editor. (IRL Press Ltd., Oxford). pp. 113–151.
3. Calvert, R., and P. Pothier. 1990. Migration of fetal intestinal intervillous cells in neonatal mice. *Anat. Rec.* 227:199–206.
4. Chandrasekaran, C., and J. I. Gordon. 1993. Cell lineage-specific and differentiation-dependent patterns of CCAAT/enhancer binding protein-α expression in the gut epithelium of normal, mutant, and transgenic mice. *Proc. Natl. Acad. Sci. USA.* 90:8871–8875.
5. Cheng, H. 1974*a*. Origin, differentiation and renewal of the four main epithelial cell types in the mouse small intestine. II. Mucous cells. *Am. J. Anat.* 141:481–502.
6. Cheng, H. 1974*b*. Origin, differentiation and renewal of the four main epithelial cell types in the mouse small intestine. IV. Paneth cells. *Am. J. Anat.* 141:521–536.
7. Cheng, H., and C. P. Leblond. 1974*a*. Origin, differentiation and renewal of the four main epithelial cell types in the mouse small intestine. I. Columnar cells. *Am. J. Anat.* 141:461–480.
8. Cheng, H., and C. P. Leblond. 1974*b*. Origin, differentiation and renewal of the four main epithelial cell types in the mouse small intestine. III. Enteroendocrine cells. *Am. J. Anat.* 141:503–520.
9. Cheng, H., and M. Bjerknes. 1985. Whole population cell kinetics and postnatal development of the mouse intestinal epithelium. *Anat. Rec.* 211:420–426.
10. Chomczynski, P., and N. Sacchi. 1987. Single-step method of RNA isolation by acid guanidinium thiocyanate-phenol-chloroform extraction. *Anal. Biochem.* 163:156–159.
11. Cohn, S. M., and M. W. Lieberman. 1984. The use of antibodies to 5′-bromo-2′deoxyuridine for the isolation of DNA sequences containing excision-repair sites. *J. Biol. Chem.* 259:12456–12462.
12. Cohn, S. M., T. C. Simon, K. A. Roth, E. H. Birkenmeier, and J. I. Gordon. 1992. Use of transgenic mice to map *cis*-acting elements in the intestinal fatty acid binding protein gene (*Fabpi*) that control its cell lineage-specific and regional patterns of expression along the duodenal-colonic and crypt-villus axes of the gut epithelium. *J. Cell Biol.* 119:27–44.
13. Demmer, L. A., M. S. Levin, J. Elovson, M. A. Reuben, A. J. Lusis, and J. I. Gordon. 1986. Tissue-specific expression and developmental regulation of the rat apolipoprotein B gene. *Proc. Natl. Acad. Sci. USA.* 83: 8102–8106.
14. Demmer, L. A., E. H. Birkenmeier, D. A. Sweetser, M. S. Levin, S. Zollman, R. S. Sparkes, T. Mohandas, A. J. Lusis, and J. I. Gordon. 1987. The cellular retinol binding protein II gene: sequence analysis of the rat gene, chromosomal localization in mice and humans, and documentation of its close linkage to the cellular retinol binding protein gene. *J. Biol. Chem.* 262:2458–2467.
15. Devereaux, J., P. Haeberli, and O. Smithies. 1984. A comprehensive set of sequence analysis programs for the VAX. *Nucleic Acids Res.* 12: 387–395.
16. Faisst, S., and S. Meyer. 1992. Compilation of vertebrate-encoded transcription factors. *Nucleic Acids Res.* 20:3–26.
17. Falk, P., K. A. Roth, and J. I. Gordon. 1994. Lectins are sensitive tools for defining differentiation programs of mouse gut epithelial cell lineages. *Am. J. Physiol. (Gastrointest. Liver Physiol).* 266:G987–G1003.
18. Feinberg, A. P., and B. Vogelstein. 1984. A technique for radiolabeling restriction endonuclease fragments to high specific activity. *Anal. Biochem.* 132:6–13.
19. Fujii, H., M. Nomura, T. Kanda, O. Amano, S. Iseki, K. Hatakeyama, and T. Ono. 1993. Cloning of a cDNA encoding rat intestinal 15 kDa protein and its tissue distribution. *Biochem. Biophys. Res. Commun.* 190: 175–180.
20. Gantz, I., S. F. Nothwehr, M. Lucey, J. C. Sacchettini, J. DelValle, L. J. Banaszak, M. Naud, J. I. Gordon, and T. Yamada. 1989. Gastrotropin: not an enterooxyntin but a member of a family of cytoplasmic hydrophobic ligand binding proteins. *J. Biol. Chem.* 264:20248–20254.
21. Ghosh, D. 1990. A relational database of transcription factors. *Nucleic Acids Res.* 18:1749–1756.
22. Gordon, J. I., G. H. Schmidt, and K. A. Roth. 1992. Studies of intestinal stem cells using normal, chimeric and transgenic mice. *FASEB (Fed. Am. Soc. Exp. Biochem.) J.* 6:3039–3050.
23. Gossler, A., T. Doetschman, R. Korn, E. Serfling, and R. Kemler. 1986. Transgenesis by means of blastocyte-derived embryonic stem cell lines. *Proc. Natl. Acad. Sci. USA.* 83:9065–9069.
24. Green, R. P., S. M. Cohn, J. C. Sacchettini, K. E. Jackson, and J. I. Gordon. 1992. The mouse intestinal fatty acid binding protein genes: nucleotide sequence, pattern of developmental and regional expression, and proposed structure of its protein product. *DNA Cell Biol.* 11:31–41.
25. Hagemann, R. F., C. P. Sigdestad, and S. Lesher. 1970. A quantitative description of the intestinal epithelium of the mouse. *Am. J. Anat.* 129:41–52.
26. Hauft, S. M., D. A. Sweetser, P. S. Rotwein, R. Lajara, P. C. Hoppe, E. H. Birkenmeier, and J. I. Gordon. 1989. A transgenic mouse model that is useful for analyzing cellular and geographic differentiation of the intestine during development. *J. Biol. Chem.* 264:8419–8429.
27. Hendry, J. H. 1993. Quantitation of intestinal clonogens by regeneration following cytotoxicity. *Sem. Develop. Biol.* 4:303–312.
28. Henning, S. J. 1987. Functional development of the gastrointestinal tract. *In* Physiology of the Gastrointestinal Tract. 2nd ed., Vol. 1. L. R. Johnson, J. Christensen, E. D. Jacobson, M. J. Jackson, and J. H. Walsh, editors. pp. 285–300. Raven Press, New York.
29. Hermiston, M. L., R. P. Green, and J. I. Gordon. 1993. Chimeric-transgenic mice represent a powerful tool for studying how the proliferation and differentiation programs of intestinal epithelial cell lineages are regulated. *Proc. Natl. Acad. Sci. USA.* 90:8866–8870.
30. Hogan, B., F. Costantini, and E. Lacey. 1986. Manipulating the Mouse Embryo: A Laboratory Manual. Cold Spring Harbor Laboratory, Cold Spring Harbor, NY. pp. 157–173.
31. Hoppler, S., and M. Bienz. 1994. Specification of a single cell type by a *Drosophila* homeotic gene. *Cell.* 76:689–702.
32. Hunt, C. R., J. H. S. Ro, D. E. Dobson, H. Y. Min, and B. M. Spiegelman. 1986. Adipocyte P2 gene: developmental expression and homology of 5′-flanking sequences among fat cell-specific genes. *Proc. Natl. Acad. Sci. USA.* 83:3786–3790.
33. Immerglück, K., P. A. Lawrence, and M. Bienz. 1990. Induction across germ layers in *Drosophila* mediated by a genetic cascade. *Cell.* 62: 261–268.
34. Kanda, T., S. Odani, M. Tomoi, Y. Matsubara, and T. Ono. 1991. Primary structure of a 15-kDa protein from rat intestinal epithelium: sequence similarity to fatty-acid-binding proteins. *Eur. J. Biochem.* 197:759–768.
35. Kedinger, M., P. M. Simon-Assmann, B. Lacroix, A. Marxer, H. P. Hauri, and K. Haffen. 1986. Fetal gut mesenchyme induces differentiation of cultured intestinal endodermal and crypt cells. *Dev. Biol.* 113:474–483.
36. Kim, S. H., K. A. Roth, A. R. Moser, and J. I. Gordon. 1993. Transgenic mouse models that explore the multistep hypothesis of intestinal neoplasia. *J. Cell Biol.* 123:877–893.
37. Kramer, W., F. Girbig, U. Gutjahr, S. Kowalewski, K. Jouvenal, G. Müller, D. Tripier, and G. Wess. 1993. Intestinal bile acid absorption: $Na^+$-dependent bile acid transport activity in rabbit small intestine correlates with the coexpression of an integral 93-kDa and a peripheral 14-kDa bile acid-binding membrane protein along the duodenum-ileum axis. *J. Biol. Chem.* 269:18035–18046.
38. Laemmli, U. K. 1970. Cleavage of structural proteins during the assembly of the head of bacteriophage T4. *Nature (Lond.).* 227:680–685.
39. Loeffler, M., and B. Grossmann. 1991. A stochastic branching model with formation of subunits applied to the growth of intestinal crypts. *J. Theor. Biol.* 150:175–191.
40. Loeffler, M., R. Stein, H. E. Wichmann, C. S. Potten, P. Kaur, and S. Chwalinski. 1986. Intestinal cell proliferation. I. A comprehensive model of steady-state proliferation in the crypt. *Cell Tiss. Kinet.* 19:627–645.
41. Loeffler, M., A. Birke, D. Winton, and C. Potten. 1993. Somatic mutation, monoclonality, and stochastic models of stem cell organization in the intestinal crypt. *J. Theor. Biol.* 160:471–491.
42. Lowe, J. B., J. C. Sacchettini, M. Laposata, J. J. McQuillan, and J. I. Gordon. 1987. Expression of rat intestinal fatty acid binding protein in *E. coli*: purification and comparison of its ligand binding characteristics with that of *E. coli*-derived rat liver fatty acid binding protein. *J. Biol. Chem.* 262:5931–5937.
43. Malo, C., and D. Ménard. 1983. Synergistic effects of insulin and thyroxine on the differentiation and proliferation of epithelial cells of the suckling mouse small intestine. *Biol. Neonat.* 44:177–184.
44. Markowitz, A. J., G. D. Wu, E. H. Birkenmeier, and P. G. Traber. 1993. The human sucrase-isomaltase gene directs complex patterns of gene expression in transgenic mice. *Am. J. Physiol.* 265 (*Gastrointest. Liver Physiol.* 28):G526–G539.
45. McKeel, D. W., Jr., and F. B. Askin. 1978. Ectopic hypophyseal hormonal cells in benign cystic teratoma of the ovary. *Arch. Pathol. Lab. Med.* 102:122–128.

46. Meinzer, H. P., B. Sandblad, and H. J. Baur. 1992. Generation-dependent control mechanisms in cell proliferation and differentiation: the power of two. *Cell Proliferation*. 25:125–140.
47. Melton, D. A., P. A. Krieg, M. R. Rebagliati, T. Maniatis, and M. R. Green. 1984. Efficient in vitro synthesis of biologically active RNA and RNA hybridization probes from plasmids containing a bacteriophage SP6 promoter. *Nucleic Acids Res.* 12:7035–7056.
48. Moore, D. D., A. R. Marks, D. I. Buckley, G. Kapler, F. Payvar, and H. M. Goodman. 1985. The first intron of the human growth hormone gene contains a binding site for glucocorticoid receptor. *Proc. Natl. Acad. Sci. USA*. 82:699–702.
49. O'Conner, T. M. 1966. Cell dynamics in the intestine of the mouse from late fetal life to maturity. *Am. J. Anat.* 118:525–536.
50. Panganiban, G. E. F., R. Reuter, M. P. Scott, and F. M. Hoffmann. 1990. A *Drosophila* growth factor homolog, decapentaplegic, regulates homeotic gene expression within and across germ layers during midgut morphogenesis. *Development (Camb.)*. 110:1041–1050.
51. Paulus, U., M. Loeffler, J. Zeidler, G. Owen, and C. S. Potten. 1993. The differentiation and lineage development of goblet cells in the murine small intestinal crypt: experimental and modelling studies. *J. Cell Sci.* 106: 473–484.
52. Peterson, G. L. 1979. A simplification of the protein assay method of Lowry et al. which is more generally applicable. *Anal. Biochem.* 83: 346–356.
53. Potten, C. S., and M. Loeffler. 1987. A comprehensive model of the crypts of the small intestine of the mouse provide insight into the mechanisms of cell migration and the proliferation hierarchy. *J. Theor. Biol.* 127: 381–391.
54. Potten, C. S., and M. Loeffler. 1990. Stem cells: attributes, cycles, spirals, pitfalls and uncertainties. Lessons for and from the crypt. *Development (Camb.)*. 110:1101–1020.
55. Reuter, R., G. E. F. Panganiban, F. M. Hoffmann, and M. P. Scott. 1990. Homeotic genes regulate the spatial expression of putative growth factors in the visceral mesoderm of *Drosophila* embryos. *Development (Camb.)*. 110:1031–1041.
56. Roth, K. A., J. M. Hertz, and J. I. Gordon. 1990. Mapping enteroendocrine cell populations in transgenic mice reveals an unexpected degree of complexity in cellular differentiation within the gastrointestinal tract. *J. Cell Biol.* 110:1791–1801.
57. Roth, K. A., E. H. Rubin, E. H. Birkenmeier, and J. I. Gordon. 1991*a*. Expression of liver fatty acid binding protein/human growth hormone fusion genes within the enterocyte and enteroendocrine cell populations of fetal transgenic mice. *J. Biol Chem.* 266:5949–5954.
58. Roth, K. A., M. L. Hermiston, and J. I. Gordon. 1991*b*. Use of transgenic mice to infer the biological properties of small intestinal stem cells and to examine the lineage relationships of their descendants. *Proc. Natl. Acad. Sci. USA*. 88:9407–9411.
59. Roth, K. A., S. M. Cohn, D. C. Rubin, J. F. Trahair, M. R. Neutra, and J. I. Gordon. 1992*a*. Regulation of gene expression in differentiating gastric epithelial cell populations of fetal, neonatal, and adult transgenic mice. *Am. J. Physiol.* 263 (*Gastrointest. Liver Physiol.* 26):G186–G197.
60. Roth, K. A., S. Kim, and J. I. Gordon. 1992*b*. Immunocytochemical studies suggest two pathways for enteroendocrine cell differentiation in the colon. *Am. J. Physiol.* 263 (*Gastrointest. Liver Physiol.* 26):G174–G180.
61. Rottman, J. N., and J. I. Gordon. 1993. Comparison of the patterns of expression of rat intestinal fatty acid binding protein/human growth hormone fusion genes in cultured intestinal epithelial cell lines and in the gut epithelium of transgenic mice. *J. Biol. Chem.* 268:11994–12002.
62. Rubin, D. C., K. A. Roth, E. H. Birkenmeier, and J. I. Gordon. 1991. Epithelial cell differentiation in normal and transgenic mouse intestinal isografts. *J. Cell Biol.* 113:1183–1192.
63. Rubin, D. C., E. Swietlicki, K. A. Roth, and J. I. Gordon. 1992. Use of fetal intestinal isografts from normal and transgenic mice to study the programming of positional information along the duodenal-to-colonic axis. *J. Biol. Chem.* 267:15122–15133.
64. Sacchettini, J. C., S. M. Hauft, S. L. Van Camp, D. P. Cistola, and J. I. Gordon. 1990. Developmental and structural studies of an intracellular lipid binding protein expressed in the ileal epithelium. *J. Biol Chem.* 265:19199-19207.
65. Sambrook, J., E. F. Fritsch, and T. Maniatis. 1989. Molecular Cloning: A Laboratory Manual. Cold Spring Harbor Laboratory, Cold Spring Harbor, NY. pp. 13–16.
66. Sanger, F., S. Nicklen, and A. R. Coulson. 1977. Use of DNA polymerase I primed by a synthetic oligonucleotide to determine a nucleotide sequence in phage fl DNA. *Proc. Natl. Acad. Sci. USA*. 74:5463–5467.
67. Schmidt, G. H., M. M. Wilkinson, and B. A. J. Ponder. 1985. Cell migration pathway in the intestinal epithelium: an in situ marker system using mouse aggregation chimeras. *Cell*. 40:425–429.
68. Schmidt, G. H., D. J. Winton, and B. A. J. Ponder. 1988. Development of the pattern of cell renewal in the crypt villus unit of chimeric mouse intestine. *Development (Camb.)*. 103:785–790.
69. Seeburg, P. H. 1982. The human growth hormone gene family: nucleotide sequences show recent divergence and predict a new polypeptide hormone. *DNA*. 1:239–249.
70. Simon, T. C., K. A. Roth, and J. I. Gordon. 1993. Use of transgenic mice to map *cis*-acting elements in the liver fatty acid-binding protein gene (*Fabpl*) that regulate its cell lineage-specific, differentiation-dependent, and spatial patterns of expression in the gut epithelium and in the liver acinus. *J. Biol Chem.* 268:18345–18358.
71. Sugii, S., E. A. Kabat, and H. H. Baer. 1982. Further immunocytochemical studies on the combining sites of *Lotus tetragonolobus* and *Ulex europaeus* I and II. *Carbohydr. Res.* 99:99–101.
72. Sweetser, D. A., J. B. Lowe, and J. I. Gordon. 1986. The nucleotide sequence of the rat liver fatty acid binding protein gene: evidence that exon 1 encodes an oligopeptide domain shared by a family of proteins which bind hydrophobic ligands. *J. Biol. Chem.* 261:5553–5561.
73. Sweetser, D. A., E. H. Birkenmeier, I. J. Klisak, S. Zollman, R. S. Sparkes, T. Mohandas, A. J. Lusis, and J. I. Gordon. 1987. The human and rodent intestinal fatty acid binding protein genes: a comparative analysis of their structure, expression and linkage relationships. *J. Biol. Chem.* 262:16060–16071.
74. Sweetser, D. A., S. M. Hauft, P. C. Hoppe, E. H. Birkenmeier, and J. I. Gordon. 1988. Transgenic mice containing intestinal fatty acid binding protein/human growth hormone fusion genes exhibit correct regional and cell specific expression of the reporter in their small intestine. *Proc. Natl. Acad. Sci. USA*. 85:9611–9615.
75. Sweetser, D. A., E. H. Birkenmeier, P. C. Hoppe, D. W. McKeel, and J. I. Gordon. 1988. Mechanisms underlying generation of gradients in gene expression within the intestine: an analysis using transgenic mice containing fatty acid binding protein/human growth hormone fusion genes. *Genes & Dev.* 2:1318–1332.
76. Tepass, U. and V. Hartenstein. 1994. Epithelium formation in the *Drosophila* midgut depends on the interaction of endoderm and mesoderm. *Development (Camb.)*. 120:579–590.
77. Trahair, J., M. Neutra, and J. I. Gordon. 1989. Use of transgenic mice to study the routing of secretory proteins in intestinal epithelial cells: analysis of human growth hormone compartmentation as a function of cell type and differentiation. *J. Cell Biol.* 19:3231–3242.
78. Winton, D. J., M. A. Blount, and B. A. J. Ponder. 1988. A clonal marker induced by mutation in mouse intestinal epithelium. *Nature (Lond.)*. 333:463–466.
79. Winton, D. J., and B. A. J. Ponder. 1990. Stem cell organization in mouse small intestine. *Proc. R. Soc. Lond. B*. 241:13–18.
80. Winton, D. 1993. Mutation induced clonal markers from polymorphic loci: application to stem cell organization in the mouse intestine. *Sem. Dev. Biol.* 4:293–302.
81. Wong, M. H., P. Oelkers, A. L. Craddock, and P. A. Dawson. 1994. Expression cloning and characterization of the hamster ileal sodium-dependent bile acid transporter. *J. Biol. Chem.* 269:1340–1347.
82. Wright, N. A., and M. Irwin. 1982. The kinetics of villus cell populations in the mouse small intestine: normal villi—the steady state requirement. *Cell Tissue Kinet.* 15:595–609.